

RESEARCH ARTICLE

Regulatory logic driving stable levels of *defective proventriculus* expression during terminal photoreceptor specification in flies

Jenny Yan^{1,*}, Caitlin Anderson¹, Kayla Viets¹, Sang Tran¹, Gregory Goldberg^{2,‡}, Stephen Small² and Robert J. Johnston, Jr^{1,§}

ABSTRACT

How differential levels of gene expression are controlled in post-mitotic neurons is poorly understood. In the *Drosophila* retina, expression of the transcription factor Defective Proventriculus (Dve) at distinct cell type-specific levels is required for terminal differentiation of color- and motion-detecting photoreceptors. Here, we find that the activities of two *cis*-regulatory enhancers are coordinated to drive *dve* expression in the fly eye. Three transcription factors act on these enhancers to determine cell-type specificity. Negative autoregulation by Dve maintains expression from each enhancer at distinct homeostatic levels. One enhancer acts as an inducible backup ('dark' shadow enhancer) that is normally repressed but becomes active in the absence of the other enhancer. Thus, two enhancers integrate combinatorial transcription factor input, feedback and redundancy to generate cell type-specific levels of *dve* expression and stable photoreceptor fate. This regulatory logic may represent a general paradigm for how precise levels of gene expression are established and maintained in post-mitotic neurons.

KEY WORDS: Defective proventriculus, Shadow enhancer, Dark shadow enhancer, Rhodopsin, *Drosophila* retina, Photoreceptor, Spineless, Orthodenticle, Spalt

INTRODUCTION

Genes are expressed at distinct cell type-specific levels at different times during development. Expression is often transient, arising for short periods of time to trigger downstream regulatory pathways. For example, expression driven by the *eve* stripe 2 enhancer, perhaps the best-understood regulatory DNA element, is very short-lived, persisting for only ~15 min after the mature stripe is fully formed during embryonic development in flies (Bothma et al., 2014). By contrast, gene expression in post-mitotic neurons must be maintained on long timescales, often for the lifetime of the organism. Establishing and maintaining distinct levels of transcription factors is particularly important for neuronal fate and function across species. For example, in worms, low levels of the transcription factor MEC-3 specify the elaborate dendritic patterning of PVD pain-sensing neurons, whereas high MEC-3

determines the simple morphology of AVM and PVM touch neurons (Smith et al., 2013). Similarly, flies use differences in levels of the homeodomain transcription factor Cut to control dendritic branching complexity in sensory neuron subtypes (Grueber et al., 2003). In mice, the Hox accessory factor FoxP1 acts as a dose-dependent determinant of motor neuron subtype identity (Dasen et al., 2008). Beyond these cases, there are numerous examples of differential transcription factor expression in neuronal subtypes, such as the unique expression levels of Brn3b in ipRGC subtypes (Chen et al., 2011).

Establishing and maintaining distinct levels of gene expression for the lifetime of a neuron presents specific challenges. Regulatory mechanisms must ensure that expression levels remain within a narrow range for days and even years while providing robustness against acute perturbations caused by activity and environment. In some cases, the transcription factors that dictate cell type-specific expression levels have been identified (Corty et al., 2016), but how these regulatory inputs are interpreted by DNA elements has not been characterized. Furthermore, it is unclear how transcription factor feedback and *cis*-regulatory redundancy contribute to ensuring proper expression levels in neurons.

Expression of transcription factors at cell type-specific levels is required for the terminal specification of motion- and color-detecting photoreceptors in the *Drosophila* retina. The *Drosophila* compound eye consists of approximately 800 ommatidia, or unit eyes, each containing eight photoreceptors (PRs) (Wolff and Ready, 1993) (Fig. 1E). The outer PRs (R1-R6) express the broad spectrum-sensitive Rhodopsin 1 (Rh1) and detect motion (Hardie, 1985), whereas the inner PRs (R7 and R8) express color-sensitive Rhodopsin proteins (Rh3-Rh6) (Gao et al., 2008; Yamaguchi et al., 2010). Two ommatidial subtypes, pale (p) and yellow (y), are randomly distributed in the retina at a ratio of 35:65 (Bell et al., 2007; Franceschini et al., 1981) (Fig. 1A-D). The p subtype contains UV-sensitive Rh3 in pR7 and blue-sensitive Rh5 in pR8, whereas the y subtype contains UV-sensitive Rh4 in yR7 and green-sensitive Rh6 in yR8 (Fig. 1A-C) (Chou et al., 1996; Fortini and Rubin, 1990; Johnston and Desplan, 2010). The specification of these photoreceptor subtypes is controlled by a complex network of transcription factors and other regulators (Hsiao et al., 2013; Jukam and Desplan, 2011; Jukam et al., 2013, 2016; Mikeladze-Dvali et al., 2005; Viets et al., 2016; Wernet et al., 2006).

Differential expression of the K50 homeodomain transcription factor Defective proventriculus (Dve) is crucial for terminal specification of photoreceptors in the fly eye (Johnston et al., 2011; Thanawala et al., 2013). Dve is expressed in a unique pattern, with high levels in the outer PRs, low levels in yR7s and no expression in pR7s or R8s (Fig. 1K). High Dve in motion-detecting outer PRs represses expression of color-detecting Rh3, Rh5 and Rh6. Low levels of Dve in yR7s repress Rh3 to maintain exclusive expression of Rh4 in yR7 subtypes in the main ventral region of the retina (Fig. 1L,

¹Department of Biology, Johns Hopkins University, 3400 North Charles Street, Baltimore, MD 21218-2685, USA. ²Center for Developmental Genetics, Department of Biology, New York University, 100 Washington Square East, New York, NY 10003-6688, USA.

*Present address: Department of Genetics, Harvard Medical School, 77 Avenue Louis Pasteur, Boston, MA 02115, USA. †Present address: Laboratory of Bacteriology, The Rockefeller University, New York, NY 10065, USA.

§Author for correspondence (robertjohnston@jhu.edu)

© R.J.J., 0000-0002-5775-6218

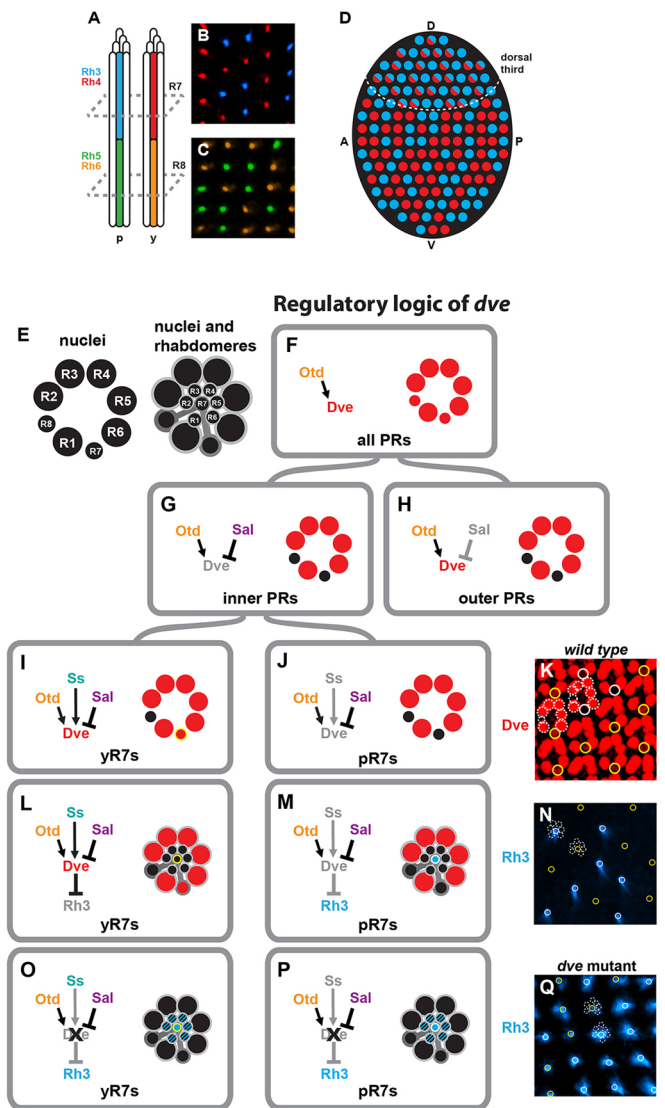


Fig. 1. The regulatory logic controlling *Dve*. (A) Rh3 (blue) and Rh4 (red) expression in pR7s and yR7s coordinates with Rh5 (green) and Rh6 (orange) expression in pR8s and yR8s in adults. (B,C) Rh3, Rh4, Rh5 and Rh6 in cross-sectional view at the levels depicted by the gray dashed lines in A. Images were taken in adult flies. (D) In the adult fly eye, two ommatidial subtypes, the Rh3-expressing pR7s (blue circles) and the Rh4-expressing yR7s (red circles), are randomly distributed in the retina at a ratio of 35:65. This mutual exclusivity in expression breaks down in the dorsal third region, where Rh3 and Rh4 are co-expressed in the γ subtype (half red/half blue circles). A, anterior; P, posterior; D, dorsal; V, ventral. (E) Nuclei and rhabdomeres of the 8 PRs (R1-8) that make up the fly ommatidium. Large outer black circles represent nuclei; smaller inner circles represent rhabdomeres. (F-J,L,M,O,P) Regulatory logic governing *dve*. (Left) Gene network. (Right) *Dve* expression pattern. Solid color represents consistent expression. Hatched colors indicate variable derepressed expression. (F) Otd activates *Dve* in all PRs. (G) Sal represses *Dve* in inner PRs. (H) The absence of Sal allows *Dve* expression in outer PRs. (I) Ss activates *Dve* in yR7s. (J) The absence of Ss prevents *Dve* expression in pR7s. (K) The interactions in F-J yield the expression pattern of *Dve*: high expression in outer PRs; low expression in yR7s; no expression in pR7s and R8s in pupae. Yellow circles indicate yR7 nuclei with *dve* on; solid white circles indicate pR7 nuclei with *dve* off; dashed white circles are nuclei of outer PRs and R8s. (L) *Dve* represses Rh3 in yR7s. (M) The absence of *Dve* allows Rh3 expression in pR7s. (N) Rh3 is expressed only in pR7s where *Dve* is absent in adults. (O-Q) In *dve* mutants, Rh3 is expressed in all R7s and variably derepressed in outer PRs in adults. (N,Q) Yellow circles indicate yR7 rhabdomeres. Solid white circles indicate pR7 rhabdomeres. Dashed white circles are rhabdomeres of outer PRs.

N). In the dorsal third, *Dve* levels are lowered further in yR7s to allow co-expression of Rh3 in Rh4-expressing cells (Fig. 1D). The absence of *Dve* expression allows expression of Rh3 in pR7s (Fig. 1M-N) and Rh5 and Rh6 in R8s (Johnston et al., 2011).

Changes in levels of *Dve* expression have a dramatic impact on Rhodopsin expression and photoreceptor fate. In *dve* null mutants, Rh3 is derepressed in all R7s, and Rh3, Rh5 and Rh6 are variably expressed in outer PRs (Fig. 1O-Q) (Johnston et al., 2011; Sood et al., 2012). In *dve* hypomorphic mutants, where levels of *Dve* are lowered but not completely lost, Rh3 is still derepressed in all R7s, but only Rh6 is expressed in outer PRs (Johnston et al., 2011). When *Dve* levels are subtly lowered upon mutation of upstream regulators, the dorsal region of Rh3 and Rh4 co-expression is expanded from one-third of the retina to the entire dorsal half (Thanawala et al., 2013). The misexpression of Rh3 in *dve* mutants causes defects in low-intensity light discrimination (Johnston et al., 2011). Deleterious effects are also seen when *Dve* levels are increased: raising levels of *Dve* in yR7s causes loss of Rh3/Rh4 co-expression in the specialized dorsal third region (Mazzoni et al., 2008; Thanawala et al., 2013), whereas overexpression in R8s represses Rh5 and Rh6 completely (Johnston et al., 2011). Thus, the differential expression of *dve* in photoreceptors is important for proper Rh expression and visual function.

Cell type-specific levels of *Dve* are achieved through regulation by the K50 homeodomain transcription factor Orthodenticle (Otd), the zinc-finger transcription factors Spalt major and Spalt related [referred to collectively as Spalt (Sal)], and the PAS-bHLH transcription factor Spineless (Ss). Otd activates *Dve* in all PRs (Fig. 1F), Sal represses *Dve* in the inner PRs (Fig. 1G-H) and Ss re-activates *Dve* in yR7s (Fig. 1I,J) (Johnston, 2013; Johnston et al., 2011).

To determine how these transcription factors dictate cell type-specific levels of *Dve* expression, we analyzed the *cis*-regulatory logic controlling *dve* and identified two enhancers, *yR7 enh* and *outer enh*, that together induced expression recapitulating endogenous *Dve* expression. *yR7 enh* is activated by Ss, Sal and Otd in yR7 cells, whereas *outer enh* is activated by Otd in all PRs and repressed by Sal in inner PRs. Negative feedback by *Dve* onto both enhancers maintains proper levels of *Dve* expression. This autoregulation is particularly important for *yR7 enh*, which is dramatically upregulated in yR7s when *Dve* feedback is ablated. Interestingly, we also observed derepression of *yR7 enh* in outer PRs in *dve* mutants, suggesting that *yR7 enh* serves as an inducible backup or ‘dark’ shadow enhancer in these cells. Shadow enhancers are DNA elements that drive redundant expression patterns and ensure robust gene expression in cases of genetic and environmental perturbation (Bothma et al., 2015; Frankel et al., 2010; Hong et al., 2008; Miller et al., 2014; Nolte et al., 2013; Perry et al., 2010; Wunderlich et al., 2015). *yR7 enh* represents an unusual ‘dark’ shadow enhancer as it is normally repressed and only becomes active when *Dve* driven by the primary *outer enh* is compromised. Together, the *yR7 enh* and *outer enh* integrate combinatorial transcription factor input, negative feedback and redundancy to ensure distinct cell type-specific levels of *dve* expression required for stable photoreceptor specification.

RESULTS

Two enhancers determine yR7- and outer PR-specific expression of *Dve*

The *dve* gene locus is ~65 kb with two alternative transcriptional starts driven by the *dve-A* promoter or *dve-B* promoter (Fig. 2A). Deletion of the *dve-A* promoter caused derepression of Rh3 in yR7s in the dorsal half of the retina (Fig. S1A,B), while Rh5 and Rh6 expression were unaffected (Fig. S1C). This incomplete *dve*

phenotype is consistent with a decrease in Dve levels in yR7s (Thanawala et al., 2013), suggesting that the *dve-A* promoter is required for normal Dve expression. To test the role of the *dve-B* promoter, we employed a CRISPR strategy to delete a ~1.5 kb region encompassing the *dve-B* promoter and first exon. Deletion of the *dve-B* promoter did not alter Dve-regulated Rh expression (Fig. S1D-F), suggesting that the *dve-B* promoter is not required for Dve expression. As the *dve-A* promoter is required for normal Dve expression, we used this promoter as the minimal promoter in enhancer reporters.

To identify *cis*-regulatory elements controlling *dve* expression, we generated transgenes containing 3-6 kb DNA fragments from the *dve* locus and the *dve-A* promoter driving nuclear GFP (Fig. 2A, *dve enh>GFP*). The *dve-A* promoter alone drove extremely weak GFP expression in pigment cells and R4 PRs, and therefore did not recapitulate normal Dve expression in all outer PRs and yR7s (Fig. S1H).

Two constructs drove GFP expression that together recapitulated endogenous Dve expression in midpupation [i.e. ~48 h after puparium formation (APF)]. *outer enh* drove expression in outer PRs (Fig. 2A,E), and *yR7 enh* drove expression specifically in a subset of R7s (Fig. 2A,B). This subset corresponded to yR7 fate, as 68% of R7s had strong GFP expression and perfectly co-expressed Ss (i.e. yR7s), whereas 32% had weak or no GFP and lacked Ss (i.e. pR7s) (Fig. 2B-D).

Additionally, *weak yR7 enh* drove weak expression in yR7s (Fig. 2A, Fig. S1M-O, described further below), and *dorsal R7 enh* drove expression in dorsal posterior R7s (Fig. 2A, Fig. S1P-Q). Four enhancers drove weak expression in all PRs (*all PRs enh 1-4*) (Fig. 2A, Fig. S1I-L).

Janelia Research Campus and the Vienna *Drosophila* Resource Center (VDRC) both generated lines that express Gal4 driven by fragments of the *dve* locus (Fig. 2A). Expression driven by these fragments was consistent with results from our *dve enh* reporter

constructs. GMR40E08, a ~3 kb fragment that overlaps with *outer enh*, drove strong GFP expression in outer PRs, whereas other constructs that either did not overlap or only partially overlapped with *outer enh* or *yR7 enh* did not show significant expression (Fig. 2A).

As *yR7 enh* and *outer enh* recapitulated endogenous Dve expression, we further characterized the temporal dynamics of these two enhancers. At midpupation, Dve protein is expressed strongly in outer PRs and weakly in yR7s (Johnston et al., 2011), similar to GFP expression driven by *yR7 enh* and *outer enh* (Fig. S2B,F,J). In third instar larvae, analysis of Dve protein expression was obscured by non-specific antibody staining (Fig. S2A) (Johnston et al., 2011). Although *outer enh* was not expressed, *yR7 enh* was expressed in a subset of R7s (Fig. S2E,I), suggesting that Dve is expressed in larval yR7s. In adults, Dve protein is expressed in yR7s and outer PRs (Fig. S2C,D). Similarly, *outer enh* drove GFP expression in outer PRs in adults (Fig. S2K,L). *yR7 enh* drove expression in all R7s in adults (Fig. S2G,H), suggesting that additional activators present only in the adult stage induce *yR7 enh* expression in all R7s, and that this enhancer is missing DNA elements that prevent ectopic Dve expression in adults.

Together, the spatiotemporal dynamics of these enhancers are consistent with endogenous *dve* expression. Next, we tested how upstream transcription factors control expression of these two enhancers.

yR7 enh is activated by Ss, Sal and Otd

yR7 enh drives expression in yR7 cells (Fig. 3A). Dve is expressed at lower levels in yR7s in the dorsal third, allowing IroC-induced activation of Rh3 and co-expression of Rh3 and Rh4 (Johnston et al., 2011). Similar to endogenous Dve expression, *yR7 enh* is expressed at lower levels in dorsal third (DT) yR7s when compared with the rest of the retina (Fig. 3D).

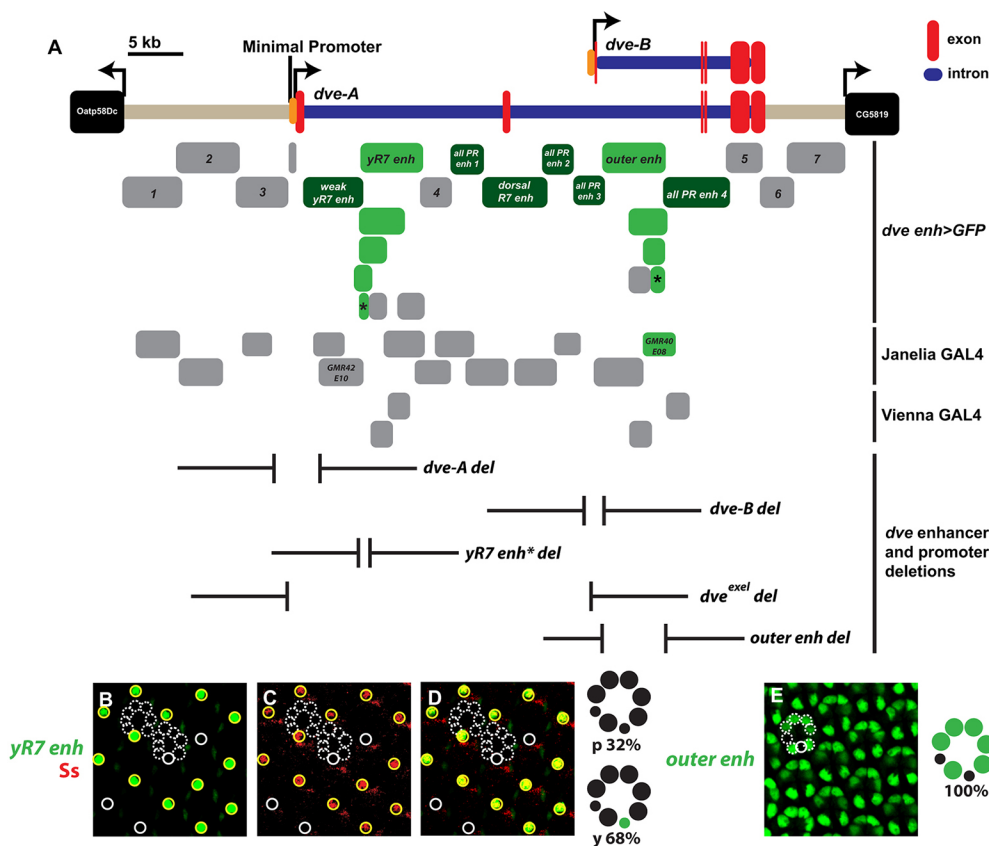


Fig. 2. Two enhancers recapitulate Dve expression. (A) The *dve* locus, reporter constructs and deletions. Reporter constructs (*dve enh>GFP*) consist of fragments of the *dve* locus and the *dve-A* promoter driving nuclear GFP. Smaller fragments, denoted with an asterisk, represent the shortest truncations generated that recapitulate the expression level of the original *dve enh>GFP* constructs. Janelia Research Campus and VDRC stocks contain fragments of the *dve* locus driving Gal4. Light green fragments drive strong expression. Dark green fragments drive weak expression. Gray fragments did not drive expression. (B-D) *yR7 enh* drives expression in yR7s at mid-pupation; Ss is a marker for yR7s. Yellow circles indicate yR7 cells; solid white circles indicate pR7 cells; dashed white circles are outer PRs and R8s. In schematics, black circles indicate no GFP expression and green circles indicate GFP expression. (E) *outer enh* constructs drive GFP expression in outer PRs at mid-pupation. Dashed white circles indicate outer PRs and R8s; solid white circle indicates R7.

Otd is required for Dve expression in *yR7s* (Johnston et al., 2011). *yR7 enh* failed to induce expression in *yR7s* in *otd* mutants, suggesting that Otd is required for activation of this enhancer (Fig. 3B).

Ss induces expression of Dve in *yR7s* (Johnston et al., 2011). Expression of *yR7 enh* was lost in *ss* mutants (Fig. 3C). Ectopic expression of Ss in all PRs induced strong *yR7 enh* expression in all *R7s* and weak expression in all other PRs (Fig. 3E), suggesting that another factor acts with Ss to activate strong *yR7 enh* expression.

As Sal is important for *R7* fate (Mollereau et al., 2001), we posited that Sal may work with Ss to activate *yR7 enh*. Expression of *yR7 enh* was completely lost in *sal* mutants (Fig. 3F), whereas ectopic expression of Sal in all PRs induced *yR7 enh* expression in a random subset of *R1* and *R6* outer PRs (Fig. 3G). We showed previously that ectopic Sal induced Ss in a random subset of *R1* and *R6* outer PRs (Johnston and Desplan, 2014). These data suggest that Ss and Sal function together to activate expression of *yR7 enh*.

Supporting our hypothesis, ectopic expression of both Ss and Sal induced strong *yR7 enh* expression in all PRs (Fig. 3H), suggesting that Ss and Sal both activate expression of *yR7 enh*. As Sal induces expression of Ss, and Ss together with Sal induces *yR7 enh*, Ss, Sal and *yR7 enh* form a coherent feed-forward loop (Fig. 3I).

To further elucidate these combinatorial regulatory interactions, we truncated *yR7 enh* to a 0.8 kb fragment (*yR7 enh**) that recapitulated *yR7* expression driven by the entire *yR7 enh* fragment (Fig. 2A; Fig. 3J,L, Fig. S3A). Three other truncations that encompass the 0.8 kb region also recapitulated *yR7* expression, whereas two truncations and four GAL4 lines generated by Janelia Research Campus and VDRC that excluded *yR7 enh** failed to drive GFP expression, consistent with the role of *yR7 enh** in driving *yR7* specific expression (Fig. 3J). *yR7 enh** contains three conserved Ss binding sites (called Xenobiotic Response Elements/XREs) (Fig. 3K), consistent with regulation by Ss.

weak yR7 enh drove weak GFP expression in *yR7s*, colocalizing with Ss expression (Fig. S1M–O). *weak yR7 enh* and *yR7 enh** share a ~250 bp overlap that contains one of the three Ss XRE binding sites (Fig. 3J,K), suggesting that while the shared XRE site can drive GFP in *yR7s*, strong expression requires the presence of additional XRE sites. The *Janelia* enhancer GMR42E10 shares a ~75 bp overlap with *yR7 enh* but does not contain any Ss XRE binding sites (Fig. 3J,K). This construct failed to drive GFP expression, suggesting that at least one Ss XRE binding site is required for *yR7*-specific expression.

To further test the roles of Ss XRE binding sites, we generated a *yR7 enh** construct that replaces all GCGTG Ss XRE binding sites with AAAAA. This construct showed a near complete loss of *yR7* GFP expression, indicating the importance of these sites for Ss activation (Fig. 3M). Very low-level expression of this reporter suggests the presence of additional cryptic Ss sites within *yR7 enh** (Fig. 3M). Searching *yR7 enh** for low-affinity Ss binding motifs (Zhu et al., 2011), we identified two putative sites (GTCTGA and GTGTGA), one of which is conserved (GTCTGA), suggesting that these cryptic/low-affinity sites may drive very low level expression in the absence of core conserved (GCGTG) sites. Together, these data suggest that Ss directly binds the XRE sites in *yR7 enh** to regulate expression. However, we cannot rule out possible indirect mechanisms.

Although *yR7 enh** has three Ss XRE sites, this enhancer contains no predicted Sal sites (Barrio et al., 1996; Sanchez et al., 2011), suggesting that Sal regulates *yR7 enh** either directly via binding to cryptic sites or indirectly through regulation of other intermediary factors. The longer *yR7 enh* contains a Sal binding site, which may contribute to regulation. Genetic epistasis analysis supports an indirect mode of regulation by Sal (Fig. S4; see below).

*yR7 enh** is required for expression of endogenous Dve in *yR7s*, as CRISPR-generated deletion of *yR7 enh** caused a loss of Dve expression specifically in *R7s* (Figs 2A, 3N) and a corresponding upregulation of Rh3 in all PRs (Fig. 3O). Similarly, the larger *dve^{exel}* deletion, covering *yR7 enh* and the *dve-A* promoter, also resulted in Rh3 upregulation in *R7s* (Fig. 2A, Fig. S1G). Together, these results suggest that *yR7*-specific expression of Dve requires *yR7 enh*, which is activated by Ss, Sal and Otd.

Negative feedback onto *yR7 enh* determines homeostatic levels

Expression levels of Dve are precisely controlled to determine region-specific activation or repression of Rh3 in *yR7s* (Thanawala et al., 2013) (Fig. 1D). Negative feedback is a mechanism that ensures precise, homeostatic levels of gene expression. As Dve is a transcriptional repressor, we hypothesized that Dve feeds back onto *yR7 enh* to control expression levels. To test Dve for negative regulation of *yR7 enh*, Dve was expressed in all PRs at high levels causing a complete loss of *yR7 enh* expression (Fig. 4A). *yR7 enh* was expressed at higher levels in *yR7s* in *dve* mutant clones compared with wild-type clones (Fig. 4B,C,F), suggesting that Dve driven by *yR7 enh* feeds back to control levels of expression in *yR7s* (Fig. 4H).

yR7 enh is a ‘dark’ shadow enhancer for outer PR expression

In addition to *yR7s*, expression of *yR7 enh* occurred in outer PRs in *dve* mutant clones (Fig. 4D,E,G), suggesting that *outer enh* induces Dve expression to completely repress *yR7 enh* in outer PRs in normal conditions (Fig. 4I,J). As *yR7 enh* was never expressed in *pR7s* or *R8s* in wild type or in *dve* mutants (Fig. 4B–E), *yR7 enh* is only competent to drive expression in *yR7s* and outer PRs, where Dve is normally expressed.

As *outer enh* drives expression in outer PRs in normal conditions and *yR7 enh* drives expression in outer PRs in *dve* mutants, we predicted that deleting *outer enh* would cause *yR7 enh* to drive expression of endogenous *dve* in outer PRs (Fig. 4I,J). Flies with a CRISPR-mediated deletion of *outer enh* displayed expression of Dve in outer PRs (Fig. 4K) and repression of Rh3, Rh5 and Rh6 (i.e. Dve target genes) in outer PRs in 1-week-old adults (Fig. 4L,N), suggesting that *yR7 enh* drives expression in the absence of functional *outer enh*. Although Rh3 expression remained unchanged (Fig. 4M), variable derepression of Rh5 and Rh6 occurred in 4-week-old adults (Fig. 4O), suggesting that expression driven by *yR7 enh* is not sufficient to completely rescue Dve expression due to differences in levels or timing.

As *yR7 enh* can drive expression in outer PRs, *yR7 enh* is a shadow enhancer (i.e. redundant regulatory DNA element) for *outer enh*, the primary enhancer for outer PR expression. Unlike typical shadow enhancers, the *yR7 enh* shadow enhancer is repressed (‘dark’) in outer PRs under normal conditions due to negative feedback from the primary enhancer (Fig. 4I). We therefore define *yR7 enh* as a ‘dark’ shadow enhancer, as its expression in outer PRs only occurs when *outer enh* function is lost (Fig. 4J).

Otd/Dve sites play context-dependent roles in *yR7 enh*

As Otd activates and Dve represses *yR7 enh*, we next tested the regulatory roles of canonical Otd/Dve binding sites (also called K50 sites; TAATCC). *yR7 enh** contains two Otd/Dve sites, which are perfectly conserved across at least five out of six *Drosophila* species (Fig. 3K). Replacing these two sites with AAAAAA caused increased levels of GFP expression in *yR7s* (Fig. 4P), suggesting that these sites mediate repression by Dve but not activation by Otd in *yR7s*. As Otd is required for expression of *yR7 enh*, the expression of GFP in *yR7s* in the absence of optimal Otd binding

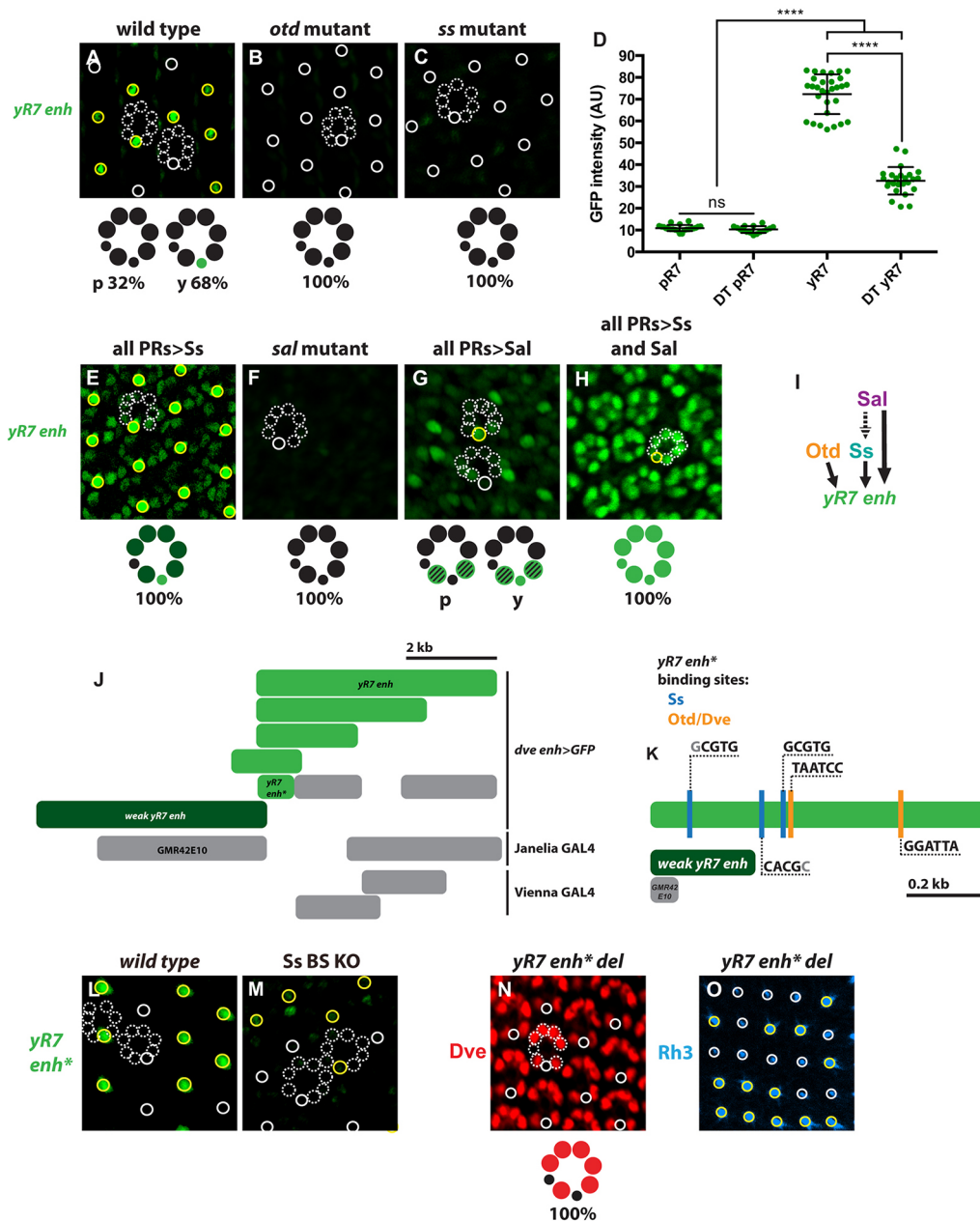


Fig. 3. *yR7 enh* is activated by Otd, Sal and Ss. (A-C, E-H, L-M) Yellow circles indicate yR7s; solid white circles indicate pR7s. Dashed white circles indicate outer PRs and R8s. Light green in ommatidium schematics indicates strong GFP expression; dark green indicates weak expression; crosshatch indicates variable expression; black indicates lack of expression. Images were acquired at mid-pupation. (A) *yR7 enh* is expressed in yR7s. (B) Expression of *yR7 enh* is lost in *otd* mutants. (C) Expression of *yR7 enh* is lost in *ss* mutants. (D) Quantification of GFP intensity in R7 cells shows three distinct intensity levels corresponding to pR7 [including pR7 and dorsal third (DT) pR7], yR7 and DT yR7 expression. Data are mean \pm s.d., $n=22$ for pR7s, 16 for DT pR7s, 31 for yR7s and 31 for DT yR7s. **** $P<0.0001$, ns indicates $P>0.05$ and not significant (unpaired t -test with Welch's correction). All measurements were internally controlled within a single mid-pupal retina. (E) *yR7 enh* is strongly expressed in all R7s and weakly expressed in all PRs when Ss is ectopically expressed in all PRs. (F) Expression of *yR7 enh* is lost in *sal* mutants (white circle indicates presumptive R7). (G) *yR7 enh* is expressed in random R1s and R6s when Sal is ectopically expressed in all PRs. (H) *yR7 enh* is expressed in all PRs when Ss and Sal are ectopically expressed in all PRs (yellow circle indicates presumptive yR7). (I) The regulatory interactions governing *yR7 enh*. Otd, Ss and Sal activate *yR7 enh*, whereas Sal activates stochastic expression of Ss in yR7s (denoted by dashed arrow). (J) A truncated 0.8 kb fragment of *yR7 enh*, indicated by *yR7 enh**, was sufficient to recapitulate GFP expression in yR7 cells. Larger truncations encompassing *yR7 enh** also expressed GFP in yR7 cells, while truncations excluding *yR7 enh** did not drive GFP expression. *weak yR7 enh* shares a ~250 bp overlap with *yR7 enh**, including one of the three Ss XRE binding sites (Fig. 3K). GMR42E10, a construct generated by *Janelia* that contains a fragment of *dve* driving Gal4, shares a ~75 bp overlap with *yR7 enh* that does not contain any Ss XRE binding sites (Fig. 3K). This construct failed to drive GFP expression in yR7 cells. Light-green fragments drive strong GFP expression; dark-green fragments drive weak GFP expression; gray fragments do not drive GFP expression. (K) *yR7 enh** contains three Ss binding sites and two Otd/Dve binding sites. Capitalized black text indicates perfect conservation across six *Drosophila* species. Capitalized gray indicates conservation across five out of the six species. Light-green fragments drive strong GFP expression; dark-green fragments drive weak GFP expression; gray fragments do not drive GFP expression. (L) *yR7 enh** is expressed in yR7s, similar to Dve and *yR7 enh*. (M) Knocking out Ss XRE binding sites in the *yR7 enh** construct resulted in a near complete loss of GFP expression. BS KO, binding site knockout. (N) CRISPR-mediated deletion of *yR7 enh* from the endogenous *dve* locus resulted in loss of Dve specifically in yR7s. Dashed white circles indicate outer PRs and R8s; solid white circles indicate R7s. Red in ommatidium schematic indicates Dve expression. (O) Loss of Dve in yR7s resulted in derepression of Rh3 in adults. Yellow circles indicate yR7s; white circles indicate pR7s; black circles indicate no expression.

sites suggests that Otd may act through additional Otd-specific cryptic sites or that activation is mediated by another activator downstream of Otd. Mutation of these sites did not cause derepression in outer PRs, suggesting that these sites mediate both repression by Dve and activation by Otd in outer PRs.

To test whether Dve directly binds the two Otd/Dve sites in *yR7 enh**, we conducted *in vitro* electrophoretic mobility shift assays (EMSAs). Dve bound sequences containing the Otd/Dve sites, and mutation of these sites dramatically decreased binding (Fig. 4Q), suggesting that Dve directly binds the two Otd/Dve sites in *yR7 enh** to repress expression.

As regulation of *yR7 enh** is dependent on Otd/Dve sites, Otd likely directly binds these sites to regulate expression. However, we cannot rule out possible indirect mechanisms.

outer enh is activated by Otd and repressed by Sal

We next characterized *outer enh*, the primary enhancer for Dve expression in outer PRs (Fig. 5A). The *dve^{exel}* deletion, which removes the first exon of *dve*, the *dve-A* promoter, and *yR7 enh*, showed no derepression of Dve target genes (Rh3, Rh5 and Rh6) in outer PRs (Fig. 2A, Fig. S1G), suggesting that *outer enh* is sufficient to drive Dve expression in outer PRs.

Otd activates Dve expression in all PRs, and Sal represses Dve expression in inner PRs (Johnston et al., 2011). *outer enh* expression was completely lost in *otd* mutants, consistent with a general requirement of Otd for *dve* expression (Fig. 5B). In *sal* mutants, *outer enh* was derepressed in inner PRs (Fig. 5C), suggesting that Sal represses this element in inner PRs. Ectopic expression of Ss in all PRs did not affect *outer enh* expression, consistent with

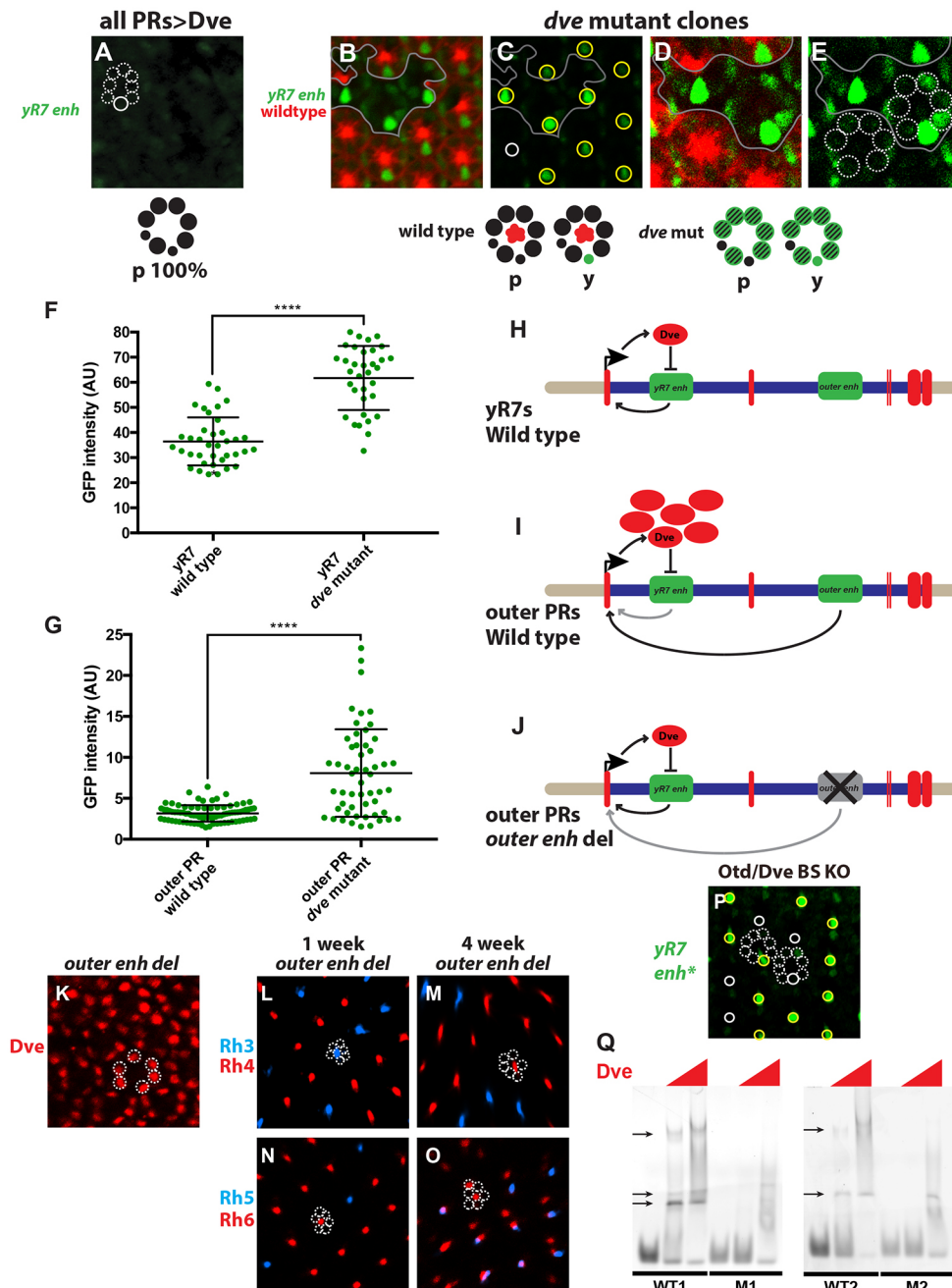


Fig. 4. See next page for legend.

Fig. 4. Dve feeds back to control *yR7 enh*. (A–E) Expression analysis was conducted on mid-pupal retinas. (A) Expression of *yR7 enh* is lost when Dve is ectopically expressed in all PRs. Dashed white circles indicate outer PRs and R8s; solid white circle indicates R7. In schematic, black circles indicate no GFP expression. (B–E) Yellow circles indicate *yR7* cells; white circles indicate *pR7* cells. Dashed white circles are outer PRs. Solid gray lines represent the boundary between *dve* mutant clones (indicated by the absence of RFP) and wild-type clones (indicated by the presence of RFP). Green in ommatidium schematic indicates strong GFP expression; crosshatching indicates variable expression; black indicates lack of expression; red spot indicates RFP expression. (B,C) In *yR7s*, *yR7 enh* is upregulated in *dve* mutant clones compared with wild-type clones. (D,E) In outer PRs, *yR7 enh* is upregulated in *dve* mutant clones compared with wild-type clones. (F) Quantification of *yR7* GFP intensity in *dve* mutant and wild-type clones. *yR7s* in *dve* mutants show greater GFP intensity than in wild-type clones. R7 cells that are GFP positive indicate *yR7s*. $n=37$ for wild-type *yR7s* and $n=37$ for *dve* mutant *yR7s*. **** $P<0.0001$, unpaired *t*-test with Welch's correction. All measurements were internally controlled within a single mid-pupal retina. (G) Quantification of GFP intensity of outer PRs in *dve* mutant and wild-type clones. In wild-type clones, outer PRs are GFP off, whereas *dve* mutant clones show a much greater distribution of GFP expression states. $n=84$ for wild-type outer PRs and $n=54$ for *dve* mutant outer PRs. **** $P<0.0001$, unpaired *t*-test with Welch's correction. All measurements were internally controlled within a single mid-pupal retina. (H) *yR7 enh* induces Dve expression that negatively feeds back onto *yR7 enh* to maintain homeostatic Dve levels in *yR7* cells. (I) *outer enh* induces Dve expression that negatively feeds back onto *yR7 enh* to completely repress *yR7* expression in outer PRs. (J) When *outer enh* function is impaired, *yR7 enh* is derepressed in outer PRs. (K) Dve remains expressed in outer PRs upon deletion of *outer enh*. Dashed white circles indicate outer PRs. (L,N) Expression of downstream Dve targets (Rh3, Rh5 and Rh6) is unaffected in *outer enh* deletion mutants in 1-week-old adults. Dashed white circles indicate outer PRs. (M,O) Variable derepression of Rh5 and Rh6 in outer PRs is observed in *outer enh* deletion mutants in 4-week-old adults. Expression of Rh3 is unaffected in *outer enh* deletion mutants in 4-week-old adults. Dashed white circles indicate outer PRs. (P) Knocking out Otd/Dve K50 binding sites resulted in an increased level of GFP in *yR7s*, suggesting that these sites mediate repression by Dve but not activation by Otd in *yR7s*. Solid yellow circles indicate *yR7s* that express GFP; solid white circles indicate *pR7s* that do not express GFP; dashed white circles indicate outer PRs and R8s. BS KO, binding site knockout. (Q) EMSAs illustrating that the binding of Dve is dependent on K50 Otd/Dve sites in *yR7 enh*. WT, wild-type sequence; M, mutation of K50 Otd/Dve site. Arrows indicate the bands shifted upon Dve binding. Multiple bands are observed likely due to the presence of multiple functional DNA binding domains within Dve (Johnston et al., 2011), yielding higher-order DNA/protein structures.

regulation of this element independent of Ss (Fig. 5D). Thus, combinatorial regulation involving activation by Otd in all PRs and repression by Sal in inner PRs yields the outer PR-specific expression of *outer enh* (Fig. 5E).

We truncated *outer enh* to a 1.3 kb fragment (*outer enh**) that recapitulated the expression of the entire *outer enh* fragment (Figs 2A, 5A,F,H, Fig. S3B). Two larger truncations and a Janelia Gal4 construct (GMR40E08) that encompass this 1.3 kb region also recapitulated expression, whereas fragments that exclude *outer enh** failed to drive GFP, consistent with the role of *outer enh** in driving outer PR-specific expression (Fig. 5F).

*outer enh** has four K50 homeodomain consensus sites (TAATCC) for Otd and Dve (Fig. 5G) (Chaney et al., 2005). *all PR enh 4* shares a 390 bp overlap with *outer enh**, including one of the Otd/Dve binding sites, suggesting that its weak expression in all PRs may be due to the single Otd/Dve binding site functioning independently of the repressive Sal input that regulates the entire *outer enh**.

We generated an *outer enh** construct that removes all TAATCC Otd/Dve binding sites by replacing them with AAAAAA (Fig. 5I). This construct showed a near complete loss of GFP expression in outer PRs, consistent with our model that Otd is required for *outer*

enh activation. As regulation of *outer enh** is dependent on Otd/Dve sites, Otd likely directly binds these sites to regulate expression. However, we cannot rule out possible indirect mechanisms.

Although *outer enh** has four Otd/Dve sites, this enhancer contains no predicted Sal sites (Barrio et al., 1996; Sanchez et al., 2011), suggesting that Sal regulates *outer enh** either directly via binding to cryptic sites or indirectly through regulation of other intermediary factors. The longer *outer enh* contains a Sal binding site, which may contribute to regulation.

Feedback onto *outer enh* determines homeostatic levels

As *yR7 enh* is controlled by negative autoregulation, we next tested whether feedback also determines expression levels driven by *outer enh*. As *outer enh* (and Dve) are highly expressed in outer PRs, we expected that *dve* mutants may exhibit subtle increases in expression from *outer enh*. Indeed, in *dve* mutant clones, *outer enh* was expressed at higher levels in outer PRs compared with wild-type clones (Fig. 6B–D). To confirm negative feedback onto *outer enh*, Dve was ectopically expressed in all PRs at high levels (*all PRs>dve*), causing a complete loss of *outer enh* expression (Fig. 6A). Thus, Dve driven by *outer enh* feeds back onto this enhancer to autoregulate and ensure homeostatic levels of expression in outer PRs (Fig. 6E).

To test whether Dve directly binds the four Otd/Dve sites in *outer enh**, we conducted EMSAs. Dve bound sequences containing the Otd/Dve sites, and mutation of these sites dramatically decreased binding (Fig. 6F), suggesting that Dve directly binds the four Otd/Dve sites in *outer enh** to repress expression.

Sal represses *outer enh* to allow Ss-mediated activation of *yR7 enh*

yR7 enh is highly sensitive to levels of Dve feedback, particularly in outer PRs where Dve levels are high. Ss alone is sufficient to induce *yR7 enh* expression at high levels in all R7s but not outer PRs (Fig. 3E). Ss and Sal together are sufficient to induce *yR7 enh* at high levels in outer PRs (Fig. 3H). As Dve driven by *outer enh* feeds back to repress *yR7 enh* in outer PRs (Fig. 4D,E,I,J) and Sal represses Dve expression from *outer enh* (Fig. 5C), Sal may activate *yR7 enh* by repressing *outer enh*.

One prediction of this model is that ectopic Ss should be sufficient to activate *yR7 enh* at high levels in outer PRs in the absence of Dve. Indeed, when Ss is expressed at high levels in all PRs in *otd* mutants that lack Dve (Johnston et al., 2011), *yR7 enh* is activated in all PRs (Fig. S4A).

This result highlights two facets of *yR7 enh* regulation. First, Ss activates *yR7 enh*, whereas Sal represses *outer enh* to allow expression of *yR7 enh*, suggesting that Sal interacts indirectly with *yR7 enh* (Fig. S4B). Second, Ss requires Otd to activate *yR7 enh* in wild-type conditions (Fig. 3B) where Ss levels are low, whereas high levels of Ss are sufficient to override the requirement for Otd (Fig. S4A).

DISCUSSION

Dve is expressed in an intricate pattern with distinct levels in different photoreceptors. The regulation required to achieve this pattern is complex, involving two enhancers controlled by three main mechanisms: combinatorial transcription factor input, negative feedback and enhancer redundancy (Fig. 7). PR-specific Otd, inner PR-specific Sal and *yR7*-specific Ss work together to induce expression of *yR7 enh* in *yR7s* (Fig. 7A). By contrast, Otd activates *outer enh* whereas Sal represses this enhancer to yield Dve expression in outer photoreceptors (Fig. 7B).

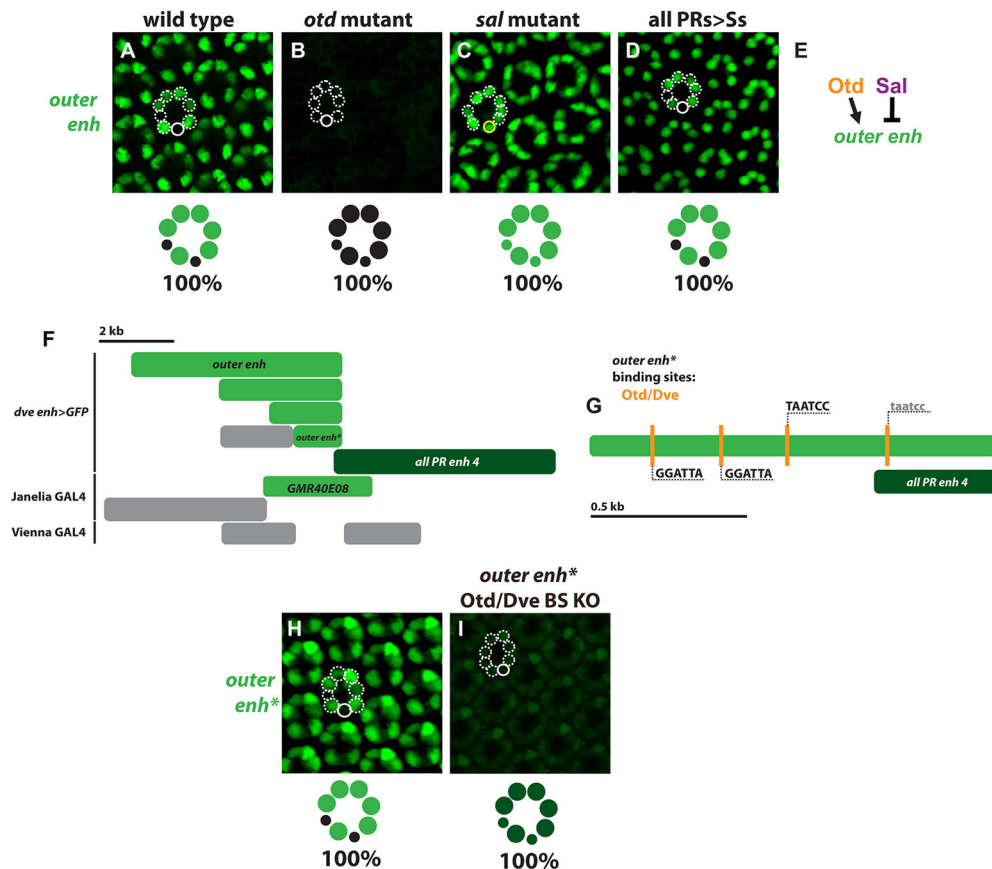


Fig. 5. *outer enhancer* is regulated by Otd and Sal. (A–D,H,I) Dashed white circles indicate outer PRs and R8s; solid white circles indicate R7s that do not express GFP; solid yellow circles indicate presumptive R7s expressing GFP. In schematics: light green circles indicate strong GFP expression; dark green circles indicate weak GFP expression; black circles indicate no GFP expression. Expression analysis was conducted on mid-pupal retinas. (A) *outer enhancer* is expressed in outer PRs. (B) Expression of *outer enhancer* is lost in *otd* mutants. (C) *outer enhancer* is expressed in all PRs in *sal* mutants. (D) Expression of *outer enhancer* is unaffected by ectopic expression of Ss in all PRs. (E) Otd activates *outer enhancer* and Sal represses *outer enhancer*. (F) A truncated 1.3 kb fragment of *outer enhancer*, denoted *outer enhancer**, was sufficient to recapitulate GFP expression in outer PRs. Larger fragments encompassing *outer enhancer** also expressed GFP in outer PRs, as did the Janelia reporter GMR40E04. Light green fragments drive strong GFP expression; dark green fragments drive weak GFP expression; gray fragments did not drive GFP expression. (G) *outer enhancer** contains three conserved Otd/Dve binding sites. Capitalized black text indicates perfect conservation across six *Drosophila* species. Lowercase gray text indicates that more than one species shows variation at the site. (H) *outer enhancer** is expressed in outer PRs, similar to Dve and *outer enhancer*. (I) Mutating Otd/Dve binding sites in *outer enhancer** resulted in a loss of expression of GFP. BS KO, binding site knockout.

Once these cell type-specific patterns are set, negative feedback by Dve maintains expression of the two enhancers at distinct levels important for regulation of downstream *rhodopsin* genes (Fig. 7C,D). This negative feedback appears especially crucial for the *yR7 enhancer*, the expression levels of which determine activation or repression of Rh3 in different regions of the retina. Gene regulatory network motifs involving negative feedback minimize variation in expression levels. With negative feedback, high concentrations of a regulator repress its expression, whereas low levels allow its activation. Negative feedback thus ensures homeostatic levels of expression (Alon, 2007; Becskei and Serrano, 2000; Irvine et al., 1993; Stewart et al., 2013).

As an additional layer of regulation, *outer enhancer* drives high levels of Dve that repress *yR7 enhancer* in outer PRs (Fig. 7E). When *outer enhancer* function is lost, *yR7 enhancer* becomes active in outer PRs, functioning as a shadow enhancer to provide redundancy and robustness to expression (Fig. 7F). Complex multi-enhancer systems enable genes to integrate multiple regulatory inputs, yielding intricate expression patterns. Although some enhancers account for distinct aspects of regulation, others drive overlapping patterns. Shadow enhancers can compensate for removal of a primary enhancer, resulting in mostly unaltered gene expression (Hong et al., 2008; Miller et al., 2014;

Nolte et al., 2013; Perry et al., 2012). These shadow enhancers provide reliability and robustness in pattern formation, allowing crucial patterning genes to be buffered against environmental and genetic variation (Barolo, 2012; Bothma et al., 2015; Frankel et al., 2010; Perry et al., 2010).

We define *yR7 enhancer* as a dark shadow enhancer, as it is normally repressed in outer PRs but becomes active when the function of the primary enhancer is impaired. We were able to identify the *yR7 enhancer* dark shadow enhancer because we were characterizing how a complex pattern was controlled by combinatorial transcription factor input and feedback acting on two enhancers. Similar to the generality of shadow enhancers (Cannavo et al., 2016), dark shadow enhancers may be a common mechanism to ensure gene expression. However, they would be challenging to identify as they are active only upon genetic or possibly environmental perturbation.

Dve is a transcriptional repressor (Johnston et al., 2011) that acts directly on *yR7 enhancer* in outer PRs to repress expression (Fig. 4Q). Generally, transcriptional repressors would likely act directly on dark shadow enhancers to repress them, poisoning them as backup systems. For transcriptional activators, more complex indirect mechanisms would be required. For example, the primary enhancer could induce the activator to activate expression of a

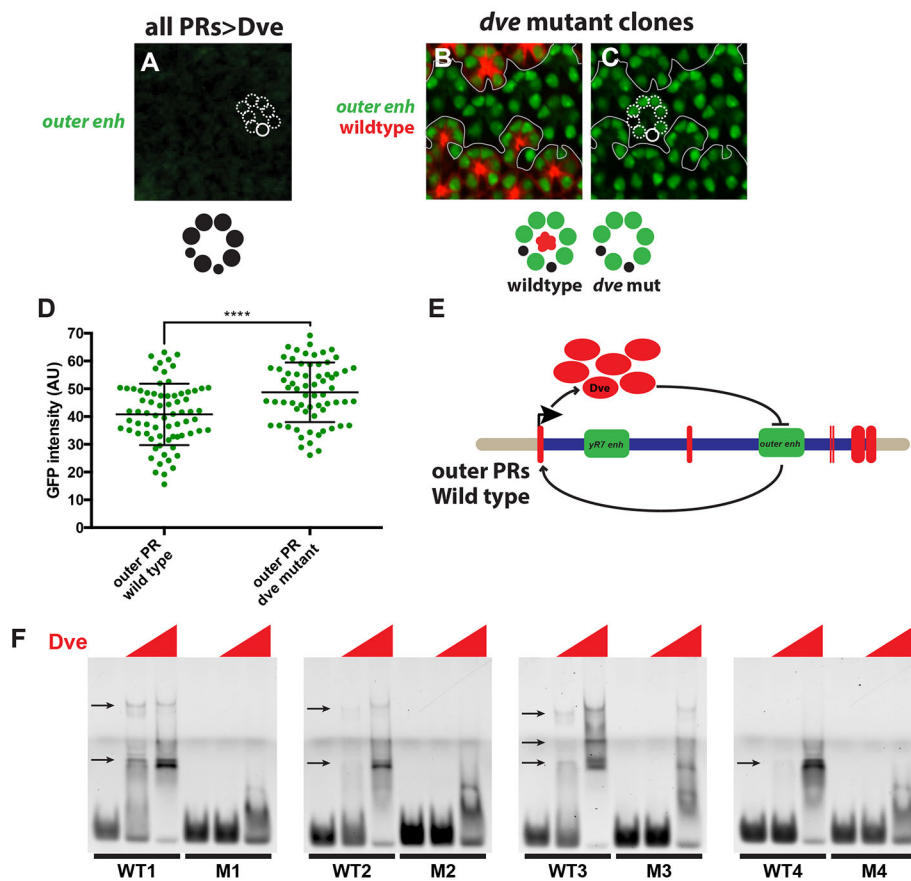


Fig. 6. Dve feeds back to control *outer enh*. (A-C) Dashed white circles indicate outer PRs and R8s; solid white circles indicate R7s. Expression analysis was conducted on mid-pupal retinas. In schematics: green circles indicate GFP expression; black circles indicate no GFP expression; red spots indicate RFP expression. (B,C) Solid gray line represents boundary between *dve* mutant clones (indicated by absence of RFP) and wild-type clones (indicated by presence of RFP). (A) Expression of *outer enh* is lost when Dve is ectopically expressed in all PRs. (B,C) Autoregulatory feedback: in outer PRs, *outer enh* is upregulated in *dve* mutant clones compared with wild-type clones. (D) Quantification of outer PR GFP expression of *outer enh* in *dve* mutant clones compared with wild-type clones. $n=72$ for wild-type outer PRs; $n=67$ for *dve* mutant outer PRs. **** $P<0.0001$, unpaired *t*-test with Welch's correction. All measurements were internally controlled within a single mid-pupal retina. (E) *outer enh* induces Dve expression that negatively feeds back onto *outer enh* to maintain homeostatic levels in outer PRs. (F) EMSAs illustrating that the binding of Dve is dependent on K50 Otd/Dve sites in *outer enh*. WT, wild-type sequence; M, mutation of K50 Otd/Dve site. Arrows indicate the bands shifted upon Dve binding. Multiple bands are observed likely due to the presence of multiple functional DNA binding domains within Dve (Johnston et al., 2011), yielding higher-order DNA/protein structures.

transcriptional repressor, which in turn could repress the dark shadow enhancer. As dark shadow enhancers require feedback, they would likely only be found in genes encoding regulatory factors.

A key aspect of regulation by primary enhancers and dark shadow enhancers is their differential responsiveness to repression. For *outer enh*, normal Dve levels induce a slight decrease in expression. However, for *yR7 enh*, these same levels completely turn off

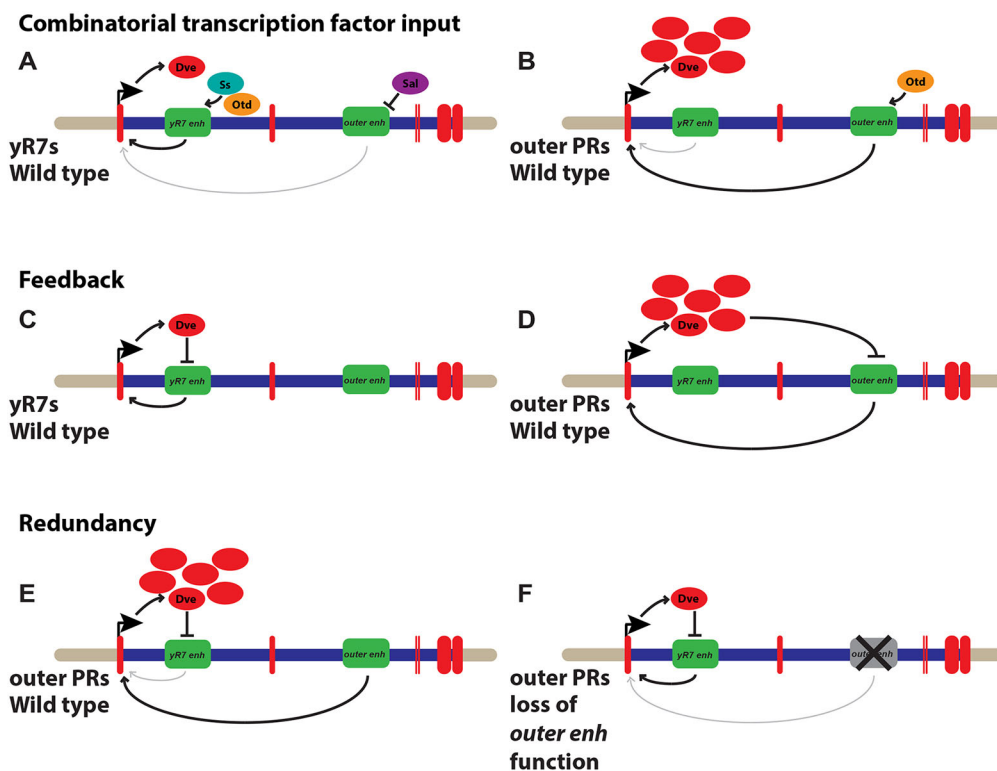


Fig. 7. Combinatorial transcription factor input, feedback and redundancy govern *dve* expression. (A) In *yR7* cells, *yR7 enh* is activated by Otd and Ss, while *outer enh* is repressed by Sal. (B) In outer PRs, Otd activates *outer enh*. (C) In *yR7* cells, *yR7 enh* induces Dve expression that negatively feeds back onto *yR7 enh* to maintain homeostatic levels. (D) In outer PRs, *outer enh* induces Dve expression that negatively feeds back onto *outer enh* to maintain homeostatic levels. (E) In wild-type outer PRs, *outer enh* induces Dve expression that negatively feeds back onto *yR7 enh* to completely repress expression. (F) Upon loss of *outer enh* function, *yR7 enh* is derepressed and drives expression in outer PRs.

expression in outer PRs. The difference may lie in activation by Otd: *outer enh* contains four Otd/Dve sites, whereas *yR7 enh* contains two (Figs 3K, 5G). As these sites mediate both activation by Otd and repression by Dve, cooperative action by the four sites in *outer enh* may drive stronger expression and prevent repression. Generally, the primary enhancer is expressed and must be significantly less susceptible to repression than the dark shadow enhancer, which is off.

Expression of Dve in outer PRs is seen in the mosquitoes *Anopheles gambiae* and *Aedes aegypti* (Johnston et al., 2011), suggesting a conserved role in Rh regulation that has been maintained over 250 million years of evolution. However, expression of Rh in R7s of mosquito species is regionalized in contrast to the stochastic pattern in *Drosophila* (Hu and Castelli-Gair, 1999), suggesting that different mechanisms have arisen to regulate Dve and Rh expression in R7s. Dark shadow enhancers may be an ancestral mechanism to ensure gene expression despite evolutionary changes. Furthermore, they may allow the evolution of new functions such as the expression of *yR7 enh* in R7s.

Dark shadow enhancers appear to provide robustness to gene expression and may act as additional mechanisms of canalization (i.e. the ability for individuals in a population to produce similar phenotypes regardless of environmental or genetic perturbation) (Waddington, 1942). Buffering of gene expression occurs at the levels of *cis*-regulatory logic (Dunipace et al., 2013; Frankel et al., 2010; Hong et al., 2008; Staller et al., 2015; Wunderlich et al., 2015) and gene networks (Cassidy et al., 2013; Lott et al., 2007; Manu et al., 2009). Dark shadow enhancers are an interesting integration of these mechanisms, whereby a primary enhancer induces expression of a factor that feeds back to repress a dark shadow enhancer. When expression from the primary enhancer is perturbed, this feedback is broken and the dark shadow enhancer becomes active. Thus, dark shadow enhancers are poised as backup mechanisms for proper gene regulation. As our understanding of complex multi-enhancer systems increases, it will be interesting to see the generality of dark shadow enhancers.

In conclusion, our studies show how two enhancers integrate combinatorial transcription factor input, negative autoregulation and redundancy in *cis*-regulatory elements to determine robust levels of gene expression in photoreceptor neurons. These mechanisms likely play roles in the establishment and maintenance of gene expression levels in other neuronal subtypes.

MATERIALS AND METHODS

Generating *dve enh>GFP* constructs

Fragments (3–6kb; Fig. 2A) were cloned into GFP reporter constructs and injected into flies. Transgenic flies were isolated and stocks were generated (see supplementary Materials and Methods and Table S1).

Drosophila strains

Flies were raised on standard cornmeal medium and grown at room temperature (25°C) (see supplementary Materials and Methods and Tables S2–S4 for complete descriptions of *Drosophila* genotypes).

CRISPR-generated deletions

dve-B promoter, *outer enh* and *yR7 enh* deletions were generated using CRISPR (see supplementary Materials and Methods and Table S5 for further details).

Otd/Dve binding site knockout

Otd/Dve binding site knockouts for *outer enh* and *yR7 enh* were generated using site-directed mutagenesis (see supplementary Materials and Methods for further details).

Electrophoretic mobility shift assay

Binding assays were performed as described previously (Johnston et al., 2011; Li-Kroeger et al., 2008) (see supplementary Materials and Methods for further details).

Antibodies

Antibodies and dilutions used were as follows: mouse anti-prospero (1:10, DSHB), rat anti-Elav (1:50, DSHB), sheep anti-GFP (1:500, Bio-Rad, 4745-1051), mouse anti-Rh3 (1:100; a gift from S. Britt, University of Colorado, Boulder, CO, USA), rabbit anti-Rh4 (1:100; a gift from C. Zuker, Columbia University, New York, USA), mouse anti-Rh5 (1:2000; Tahayato et al., 2003), rabbit anti-Rh6 (1:2000; Tahayato et al., 2003), guinea pig anti-Ss (1:200; a gift from Y. N. Jan, University of California, San Francisco, CA, USA) and rabbit anti-Dve (1:500; Nakagoshi et al., 1998). All secondary antibodies were Alexa-conjugated (1:400; Molecular Probes).

Retina dissection and immunohistochemistry

Retinas were dissected and stained as described previously (Hsiao et al., 2012) (see supplementary Materials and Methods for further details).

Quantification

Fluorescence intensity of nuclear GFP expression of single retinas was quantified using the ImageJ processing program. A small region in the center of each nucleus was selected for fluorescence intensity measurement. Images were taken under subsaturating conditions and comparisons of GFP intensity were drawn between cells of the same retina. Column scatterplots were generated using Graphpad Prism.

Acknowledgements

We are grateful to Steve Britt, Lily Jan, Yuh-Nung Jan, Hideki Nakagoshi, Charles Zuker, the Bloomington Stock Center and the Vienna *Drosophila* Resource Center (VDRC) for generously providing published fly stocks and antibodies. We thank Reiji Kuruvilla, Mike Levine, David Lorberbaum, Richard Mann and Alexandra Neuhaus-Follini for helpful comments on the manuscript.

Competing interests

The authors declare no competing or financial interests.

Author contributions

Conceptualization: J.Y., G.G., R.J.J.; Methodology: J.Y., S.T., G.G., R.J.J.; Investigation: J.Y., C.A., K.V., S.T., G.G.; Writing – original draft: J.Y., R.J.J.; Writing – review and editing: J.Y., R.J.J., S.S.; Funding acquisition: S.S., R.J.J.; Supervision: R.J.J.

Funding

R.J.J. and S.S. were supported by the National Institute of General Medical Sciences (R01GM106090-01A1/NYU F7784-01). R.J.J. was supported by a Pew Scholar Award from Pew Charitable Trusts (00027373), by a March of Dimes Foundation Basil O'Connor Scholar Award (5-FY15-21) and by the National Eye Institute (R01EY025598). Deposited in PMC for release after 12 months.

Supplementary information

Supplementary information available online at <http://dev.biologists.org/lookup/doi/10.1242/dev.144030.supplemental>

References

- Alon, U. (2007). Network motifs: theory and experimental approaches. *Nat. Rev. Genet.* **8**, 450–461.
- Barolo, S. (2012). Shadow enhancers: frequently asked questions about distributed *cis*-regulatory information and enhancer redundancy. *BioEssays* **34**, 135–141.
- Barrio, R., Shea, M. J., Carulli, J., Lipkow, K., Gaul, U., Frommer, G., Schuh, R., Jäckle, H. and Kafatos, F. C. (1996). The spalt-related gene of *Drosophila melanogaster* is a member of an ancient gene family, defined by the adjacent, region-specific homeotic gene spalt. *Dev. Genes Evol.* **206**, 315–325.
- Barrio, R., de Celis, J. F., Bolshakov, S. and Kafatos, F. C. (1999). Identification of regulatory regions driving the expression of the *Drosophila* spalt complex at different developmental stages. *Dev. Biol.* **215**, 33–47.
- Beckskei, A. and Serrano, L. (2000). Engineering stability in gene networks by autoregulation. *Nature* **405**, 590–593.
- Bell, M. L., Earl, J. B. and Britt, S. G. (2007). Two types of *Drosophila* R7 photoreceptor cells are arranged randomly: a model for stochastic cell-fate determination. *J. Comp. Neurol.* **502**, 75–85.

- Bothma, J. P., Garcia, H. G., Esposito, E., Schlissel, G., Gregor, T. and Levine, M.** (2014). Dynamic regulation of eve stripe 2 expression reveals transcriptional bursts in living *Drosophila* embryos. *Proc. Natl. Acad. Sci. USA* **111**, 10598-10603.
- Bothma, J. P., Garcia, H. G., Ng, S., Perry, M. W., Gregor, T. and Levine, M.** (2015). Enhancer additivity and non-additivity are determined by enhancer strength in the *Drosophila* embryo. *Elife* **4**.
- Brand, A. H. and Perrimon, N.** (1993). Targeted gene expression as a means of altering cell fates and generating dominant phenotypes. *Development* **118**, 401-415.
- Cannavò, E., Khouchi, P., Garfield, D. A., Geeleher, P., Zichner, T., Gustafson, E. H., Ciglar, L., Korbel, J. O. and Furlong, E. E. M.** (2016). Shadow Enhancers Are Pervasive Features of Developmental Regulatory Networks. *Curr. Biol.* **26**, 38-51.
- Cassidy, J. J., Jha, A. R., Posadas, D. M., Giri, R., Venken, K. J. T., Ji, J., Jiang, H., Bellen, H. J., White, K. P. and Carthew, R. W.** (2013). miR-9a minimizes the phenotypic impact of genomic diversity by buffering a transcription factor. *Cell* **155**, 1556-1567.
- Chaney, B. A., Clark-Baldwin, K., Dave, V., Ma, J. and Rance, M.** (2005). Solution structure of the K50 class homeodomain PITX2 bound to DNA and implications for mutations that cause Rieger syndrome. *Biochemistry* **44**, 7497-7511.
- Chen, S.-K., Badea, T. C. and Hattar, S.** (2011). Photoentrainment and pupillary light reflex are mediated by distinct populations of ipRGCs. *Nature* **476**, 92-95.
- Chou, W.-H., Hall, K. J., Wilson, D. B., Wideman, C. L., Townson, S. M., Chadwell, L. V. and Britt, S. G.** (1996). Identification of a novel *Drosophila* opsin reveals specific patterning of the R7 and R8 photoreceptor cells. *Neuron* **17**, 1101-1115.
- Corty, M. M., Tam, J. and Grueber, W. B.** (2016). Dendritic diversification through transcription factor-mediated suppression of alternative morphologies. *Development* **143**, 1351-1362.
- Dasen, J. S., De Camilli, A., Wang, B., Tucker, P. W. and Jessell, T. M.** (2008). Hox repertoires for motor neuron diversity and connectivity gated by a single accessory factor, FoxP1. *Cell* **134**, 304-316.
- Duncan, D. M., Burgess, E. A. and Duncan, I.** (1998). Control of distal antennal identity and tarsal development in *Drosophila* by spineless-aristopedia, a homolog of the mammalian dioxin receptor. *Genes Dev.* **12**, 1290-1303.
- Dunipace, L., Saunders, A., Ashe, H. L. and Stathopoulos, A.** (2013). Autoregulatory feedback controls sequential action of cis-regulatory modules at the brinker locus. *Dev. Cell* **26**, 536-543.
- Fortini, M. E. and Rubin, G. M.** (1990). Analysis of cis-acting requirements of the Rh3 and Rh4 genes reveals a bipartite organization to rhodopsin promoters in *Drosophila melanogaster*. *Genes Dev.* **4**, 444-463.
- Franceschini, N., Kirschfeld, K. and Minke, B.** (1981). Fluorescence of photoreceptor cells observed in vivo. *Science* **213**, 1264-1267.
- Frankel, N., Davis, G. K., Vargas, D., Wang, S., Payne, F. and Stern, D. L.** (2010). Phenotypic robustness conferred by apparently redundant transcriptional enhancers. *Nature* **466**, 490-493.
- Gao, S., Takemura, S. Y., Ting, C.-Y., Huang, S., Lu, Z., Luan, H., Rister, J., Thum, A. S., Yang, M., Hong, S.-T. et al.** (2008). The neural substrate of spectral preference in *Drosophila*. *Neuron* **60**, 328-342.
- Grueber, W. B., Jan, L. Y. and Jan, Y. N.** (2003). Different levels of the homeodomain protein *ect* regulate distinct dendrite branching patterns of *Drosophila* multidendritic neurons. *Cell* **112**, 805-818.
- Hardie, R. C.** (1985). Functional organization of the fly retina. In (ed. H. Autrum, D. Ottoson, E. R. Perl, R. F. Schmidt, H. Shimazu, W. D. Willis). *Progress in Sensory Physiology*. Berlin: Springer.
- Hong, J.-W., Hendrix, D. A. and Levine, M. S.** (2008). Shadow enhancers as a source of evolutionary novelty. *Science* **321**, 1314.
- Hsiao, H. Y., Johnston, R. J., Jukam, D., Vasiliauskas, D., Desplan, C. and Rister, J.** (2012). Dissection and immunohistochemistry of larval, pupal and adult *Drosophila* retinas. *J. Vis. Exp.* e4347.
- Hsiao, H.-Y., Jukam, D., Johnston, R. and Desplan, C.** (2013). The neuronal transcription factor *ect* wing regulates specification and maintenance of *Drosophila* R8 photoreceptor subtypes. *Dev. Biol.* **381**, 482-490.
- Hu, N. and Castelli-Gair, J.** (1999). Study of the posterior spiracles of *Drosophila* as a model to understand the genetic and cellular mechanisms controlling morphogenesis. *Dev. Biol.* **214**, 197-210.
- Irvine, K. D., Botas, J., Jha, S., Mann, R. S. and Hogness, D. S.** (1993). Negative autoregulation by Ultrabithorax controls the level and pattern of its expression. *Development* **117**, 387-399.
- Johnston, R. J., Jr.** (2013). Lessons about terminal differentiation from the specification of color-detecting photoreceptors in the *Drosophila* retina. *Ann. N. Y. Acad. Sci.* **1293**, 33-44.
- Johnston, R. J., Jr and Desplan, C.** (2010). Stochastic mechanisms of cell fate specification that yield random or robust outcomes. *Annu. Rev. Cell Dev. Biol.* **26**, 689-719.
- Johnston, R. J., Jr and Desplan, C.** (2014). Interchromosomal communication coordinates intrinsically stochastic expression between alleles. *Science* **343**, 661-665.
- Johnston, R. J., Jr, Otake, Y., Sood, P., Vogt, N., Behnia, R., Vasiliauskas, D., McDonald, E., Xie, B., Koenig, S., Wolf, R. et al.** (2011). Interlocked feedforward loops control cell-type-specific Rhodopsin expression in the *Drosophila* eye. *Cell* **145**, 956-968.
- Jukam, D. and Desplan, C.** (2011). Binary regulation of Hippo pathway by Merlin/NF2, Kibra, Lgl, and Melted specifies and maintains postmitotic neuronal fate. *Dev. Cell* **21**, 874-887.
- Jukam, D., Xie, B., Rister, J., Terrell, D., Charlton-Perkins, M., Pistillo, D., Gebelein, B., Desplan, C. and Cook, T.** (2013). Opposite feedbacks in the Hippo pathway for growth control and neural fate. *Science* **342**, 1238016.
- Jukam, D., Viets, K., Anderson, C., Zhou, C., DeFord, P., Yan, J., Cao, J. and Johnston, R. J., Jr.** (2016). The insulator protein BEAF-32 is required for Hippo pathway activity in the terminal differentiation of neuronal subtypes. *Development* **143**, 2389-2397.
- Kuhnlein, R. P. and Schuh, R.** (1996). Dual function of the region-specific homeotic gene *spalt* during *Drosophila* tracheal system development. *Development* **122**, 2215-2223.
- Li-Kroeger, D., Witt, L. M., Grimes, H. L., Cook, T. A. and Gebelein, B.** (2008). Hox and senseless antagonism functions as a molecular switch to regulate EGF secretion in the *Drosophila* PNS. *Dev. Cell* **15**, 298-308.
- Lott, S. E., Kreitman, M., Palsson, A., Alekseeva, E. and Ludwig, M. Z.** (2007). Canalization of segmentation and its evolution in *Drosophila*. *Proc. Natl. Acad. Sci. U. S. A.* **104**, 10926-10931.
- Manu, M., Surkova, S., Spirov, A. V., Gursky, V. V., Janssens, H., Kim, A.-R., Radulescu, O., Vanario-Alonso, C. E., Sharp, D. H., Samsonova, M. et al.** (2009). Canalization of gene expression in the *Drosophila* blastoderm by gap gene cross regulation. *PLoS Biol.* **7**, e1000049.
- Mazzoni, E. O., Celik, A., Wernet, M. F., Vasiliauskas, D., Johnston, R. J., Cook, T. A., Pichaud, F. and Desplan, C.** (2008). Iroquois complex genes induce co-expression of rhodopsins in *Drosophila*. *PLoS Biol.* **6**, e97.
- Mikeladze-Dvali, T., Wernet, M. F., Pistillo, D., Mazzoni, E. O., Telesman, A. A., Chen, Y.-W., Cohen, S. and Desplan, C.** (2005). The growth regulators *warts/flats* and *melted* interact in a bistable loop to specify opposite fates in *Drosophila* R8 photoreceptors. *Cell* **122**, 775-787.
- Miller, S. W., Rebeiz, M., Atanasov, J. E. and Posakony, J. W.** (2014). Neural precursor-specific expression of multiple *Drosophila* genes is driven by dual enhancer modules with overlapping function. *Proc. Natl. Acad. Sci. USA* **111**, 17194-17199.
- Mollereau, B., Dominguez, M., Webel, R., Colley, N. J., Keung, B., de Celis, J. F. and Desplan, C.** (2001). Two-step process for photoreceptor formation in *Drosophila*. *Nature* **412**, 911-913.
- Nakagawa, Y., Fujiwara-Fukuta, S., Yorimitsu, T., Tanaka, S., Minami, R., Shimooka, L. and Nakagoshi, H.** (2011). Spatial and temporal requirement of defective proventriculus activity during *Drosophila* midgut development. *Mech. Dev.* **128**, 258-267.
- Nakagoshi, H., Hoshi, M., Nabeshima, Y.-i. and Matsuzaki, F.** (1998). A novel homeobox gene mediates the Dpp signal to establish functional specificity within target cells. *Genes Dev.* **12**, 2724-2734.
- Noite, C., Jinks, T., Wang, X., Martinez Pastor, M. T. and Krumlauf, R.** (2013). Shadow enhancers flanking the HoxB cluster direct dynamic Hox expression in early heart and endoderm development. *Dev. Biol.* **383**, 158-173.
- O'Gorman, S., Fox, D. T. and Wahl, G. M.** (1991). Recombinase-mediated gene activation and site-specific integration in mammalian cells. *Science* **251**, 1351-1355.
- Perry, M. W., Boettiger, A. N., Bothma, J. P. and Levine, M.** (2010). Shadow enhancers foster robustness of *Drosophila* gastrulation. *Curr. Biol.* **20**, 1562-1567.
- Perry, M. W., Bothma, J. P., Luu, R. D. and Levine, M.** (2012). Precision of hunchback expression in the *Drosophila* embryo. *Curr. Biol.* **22**, 2247-2252.
- Sánchez, J., Talamillo, A., González, M., Sánchez-Pulido, L., Jiménez, S., Pirone, L., Sutherland, J. D. and Barrio, R.** (2011). *Drosophila* Sal and Salr are transcriptional repressors. *Biochem. J.* **438**, 437-445.
- Smith, C. J., O'Brien, T., Chatzigeorgiou, M., Spencer, W. C., Feingold-Link, E., Husson, S. J., Hori, S., Mitani, S., Gottschalk, A., Schafer, W. R. et al. III.** (2013). Sensory neuron fates are distinguished by a transcriptional switch that regulates dendrite branch stabilization. *Neuron* **79**, 266-280.
- Sood, P., Johnston, R. J., Jr and Kussell, E.** (2012). Stochastic de-repression of Rhodopsins in single photoreceptors of the fly retina. *PLoS Comput. Biol.* **8**, e1002357.
- Staller, M. V., Vincent, B. J., Bragdon, M. D. J., Lydiard-Martin, T., Wunderlich, Z., Estrada, J. and DePace, A. H.** (2015). Shadow enhancers enable Hunchback bifunctionality in the *Drosophila* embryo. *Proc. Natl. Acad. Sci. U. S. A.* **112**, 785-790.
- Stewart, A. J., Seymour, R. M., Pomiankowski, A. and Reuter, M.** (2013). Under-dominance constrains the evolution of negative autoregulation in diploids. *PLoS Comput. Biol.* **9**, e1002992.
- Tahayato, A., Sonnevile, R., Pichaud, F., Wernet, M. F., Papatsenko, D., Beaufils, P., Cook, T. and Desplan, C.** (2003). *Otd/Crx*, a dual regulator for the specification of ommatidia subtypes in the *Drosophila* retina. *Dev. Cell* **5**, 391-402.

- Terriente, J., Perea, D., Suzanne, M. and Diaz-Benjumea, F. J.** (2008). The *Drosophila* gene *zfh2* is required to establish proximal-distal domains in the wing disc. *Dev. Biol.* **320**, 102-112.
- Thanawala, S. U., Rister, J., Goldberg, G. W., Zuskov, A., Olesnick, E. C., Flowers, J. M., Jukam, D., Purugganan, M. D., Gavis, E. R., Desplan, C. et al., Jr.** (2013). Regional modulation of a stochastically expressed factor determines photoreceptor subtypes in the *Drosophila* retina. *Dev. Cell* **25**, 93-105.
- Vandendries, E. R., Johnson, D. and Reinke, R.** (1996). *orthodenticle* is required for photoreceptor cell development in the *Drosophila* eye. *Dev. Biol.* **173**, 243-255.
- Viets, K., Eldred, K. C. and Johnston, R. J., Jr.** (2016). Mechanisms of Photoreceptor Patterning in Vertebrates and Invertebrates. *Trends Genet.* **32**, 638-659.
- Waddington, C. H.** (1942). Canalization of development and the inheritance of acquired characteristics. *Nature* **150**, 563-565.
- Wernet, M. F., Labhart, T., Baumann, F., Mazzoni, E. O., Pichaud, F. and Desplan, C.** (2003). Homothorax switches function of *Drosophila* photoreceptors from color to polarized light sensors. *Cell* **115**, 267-279.
- Wernet, M. F., Mazzoni, E. O., Çelik, A., Duncan, D. M., Duncan, I. and Desplan, C.** (2006). Stochastic spineless expression creates the retinal mosaic for colour vision. *Nature* **440**, 174-180.
- Wolff, T. and Ready, D. F.** (1993). Pattern formation in the *Drosophila* retina. In *The Development of Drosophila Melanogaster. II.* (ed. M. Bate and A. Martinez-Arias), pp. 1277-1316. Cold Spring Harbor, NY: Cold Spring Harbor Laboratory Press.
- Wunderlich, Z., Bragdon, M. D. J., Vincent, B. J., White, J. A., Estrada, J. and DePace, A. H.** (2015). Krüppel Expression Levels Are Maintained through Compensatory Evolution of Shadow Enhancers. *Cell Rep* **12**, 1740-1747.
- Yamaguchi, S., Desplan, C. and Heisenberg, M.** (2010). Contribution of photoreceptor subtypes to spectral wavelength preference in *Drosophila*. *Proc. Natl. Acad. Sci. USA* **107**, 5634-5639.
- Zhu, L. J., Christensen, R. G., Kazemian, M., Hull, C. J., Enuameh, M. S., Basciotta, M. D., Brasfield, J. A., Zhu, C., Asriyan, Y., Lapointe, D. S. et al.** (2011). FlyFactorSurvey: a database of *Drosophila* transcription factor binding specificities determined using the bacterial one-hybrid system. *Nucleic Acids Res.* **39** Suppl. 1, D111- D117.

Supplemental Figures

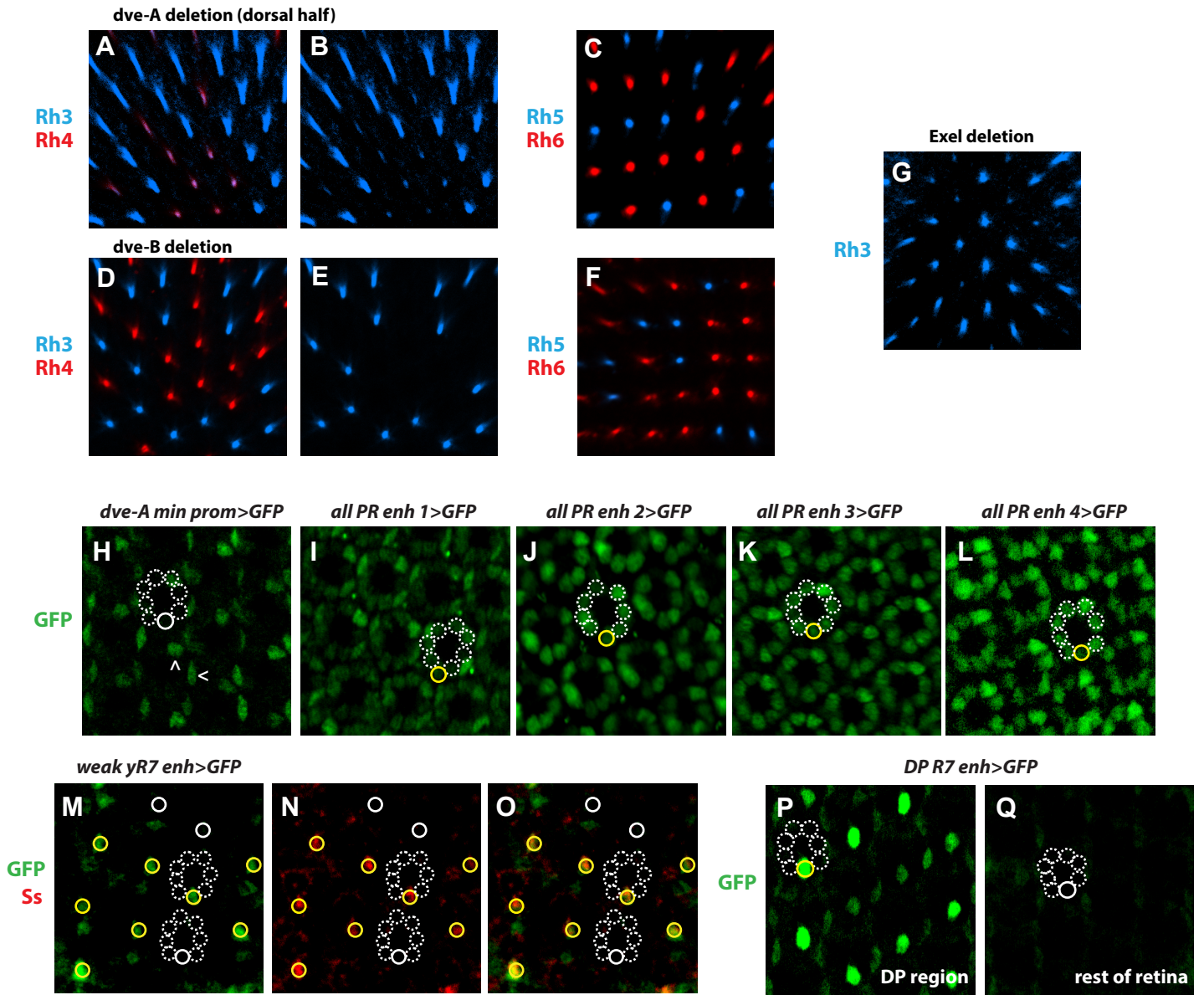


Figure S1. *dve enh>GFP* constructs and *dve-A* and *dve-B* promoter deletions

A-C. *dve-A* promoter deletion resulted in upregulation of Rh3 in all R7s in the dorsal half of the retina. Dve targets Rh5 and Rh6 displayed wild type expression.

D-F. *dve-B* promoter deletion displayed wild type expression of Dve targets (Rh3, Rh5, and Rh6).

G. *dve^{exel}* deletion, covering *yR7 enh* and the *dve-A* promoter, resulted in Rh3 upregulation in R7s.

H. *dve-A min prom* drove weak expression in R4s (denoted by ^) and pigment cells (denoted by <). Dashed white circles represent outer PRs and R8s; solid white circle indicates R7.

I-L. Four enhancers (*all PR enh 1-4*) drove weak GFP expression in all PRs. Dashed white circles represent PRs. Yellow circles denote GFP-expressing R7s.

M-O. *weak yR7 enh* displayed weak GFP expression in *yR7s*; *Ss* is a marker for *yR7s*. Dashed white circles represent outer PRs and R8s, solid white circles denote *pR7s*, and solid yellow circles denote *yR7s*.

P-Q. *dorsal R7 enh* drove expression in R7s in the dorsal posterior (DP) region of the retina. Dashed white circles represent PRs. Yellow circles indicate GFP-expressing R7; solid white circle indicates non-expressing R7.

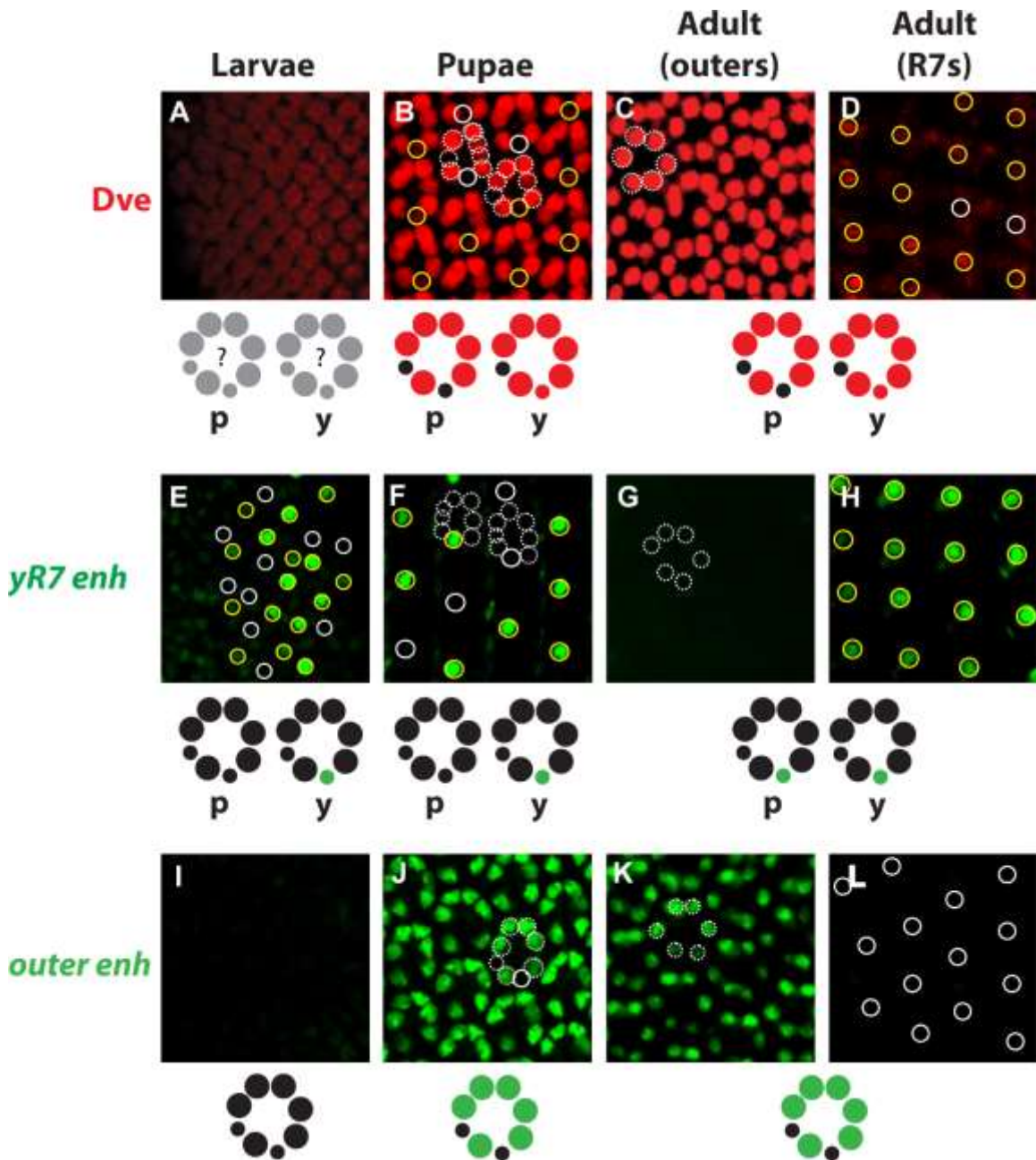


Figure S2. Differential expression of Dve throughout development

For A-L, in schematics, red circles indicate endogenous Dve expression, green circles indicate GFP expression, black circles indicate no expression (endogenous Dve or GFP), and gray circles indicate indeterminate expression.

For B-D, yellow circles indicate **yR7** cells. Solid white circles indicate **pR7** cells. Dashed white circles are outer PRs and R8s.

For E-H, yellow circles indicate **yR7** cells. Solid white circles indicate **pR7** cells. Dashed white circles are outer PRs and R8s.

For J-L, dashed white circles represent outer PRs; solid white circles indicate R7s.

A. Antibody staining for Dve is nonspecific in larvae.

B-D. Dve is highly expressed in outer PRs and weakly expressed in **yR7s** in pupae and adults.

E-F. **yR7 enh** is expressed in **yR7s** in larvae and pupae.

G-H. **yR7 enh** is expressed in all R7 cells in the adult but is not expressed in outer photoreceptors.

I. *outer enh* is not expressed in larvae.

J-L. *outer enh* drives expression in outer PRs in pupae and adults, but is not expressed in R7s.

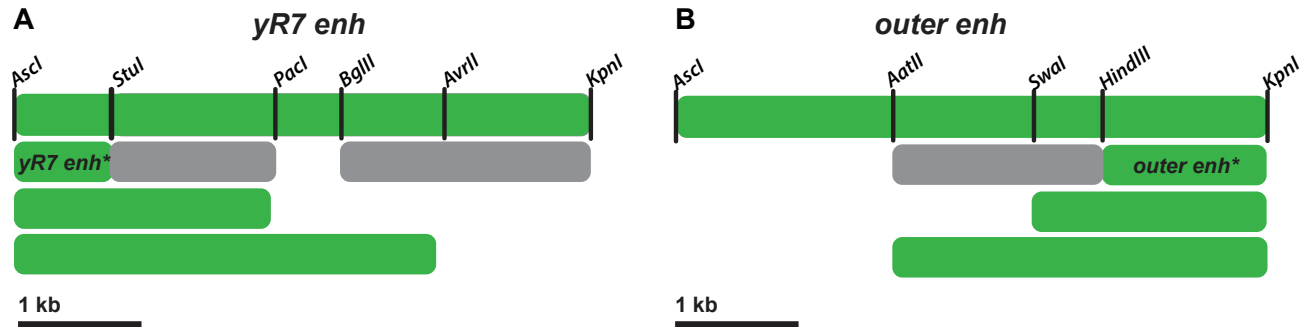


Figure S3. Restriction enzyme sites used to generate *dve enh* truncations

A. Schematic of the *yR7 enh* and the restriction enzyme sites used to generate the *yR7 enh** and other truncations.

B. Schematic of the *outer enh* and the restriction enzyme sites used to generate the *outer enh** and other truncations.

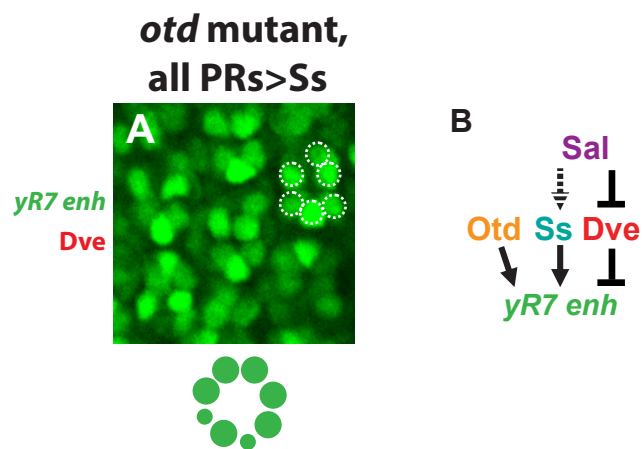


Figure S4. Sal activates *yR7 enh* by repressing *Dve*

A. In *otd* mutants, in which *Dve* is not expressed, ectopic *Ss* induces *yR7 enh* in all PRs.

B. The regulatory interactions governing *yR7 enh*. *Otd* and *Ss* activate *yR7 enh*, while *Dve* represses *yR7 enh*. *Sal* activates stochastic expression of *Ss* (denoted by dashed arrow) in *yR7s* and represses *Dve*.

Supplementary Materials and Methods

Generating *dve enh>GFP* constructs

3-6kb fragments (Fig. 2A) were amplified using DNA isolated from *yw*⁶⁷ flies and ligated into the pGEM-T easy vector. The 699 bp *dve* minimal promoter was subcloned into a pJR16 nGFPcDNA reporter vector containing a *w⁺* marker, generating the pGG14 vector. Other fragments of the *dve* locus were subcloned into pGG14 before microinjection into fly embryos. Constructs were then integrated into the genome via the attP/B system, and injected flies were crossed with a balancer stock with the genotype *yw*; *+/+*; *Tm2/Tm6b*. Red-eyed offspring were isolated, and transgenes were balanced over *Tm6b*. Primers and restriction enzymes used to generate each *dve* enhancer construct are shown in Table S1.

Enhancer constructs *yR7 enh>GFP* and *outer enh>GFP* were further truncated using restriction enzymes and blunt end ligation (Fig. S3A,B). Reporter vectors were microinjected into fly embryos, and transgenic lines were established using the same methods as above.

Drosophila strains

Flies were raised on standard cornmeal medium and grown at room temperature (25°C). Transgenic lines used include *dve* enhancer gene constructs generated for this project, as well as the reagents in Table S2.

The GAL4-UAS system was used to ectopically express *Sal*, *Ss*, and *Dve* (Brand and Perrimon, 1993), while the FLP-FRT system was used to create *sal* and *dve* mutant phenotypes (O'Gorman et al., 1991). Shortened and complete genotypes of flies examined are found in Table S3.

Janelia and VDRC Stock Centers generated transgenic lines that express GAL4 driven by flanking non-coding or intronic regions of various genes. GAL4 lines

associated with *dve yR7* and *dve outer* enhancer elements were crossed with UAS-nlsGFP. See Table S4.

CRISPR-generated deletions

dve-B promoter, *outer enh*, and *yR7 enh* deletions were generated using CRISPR. We designed four gRNAs per deletion, two flanking either side of the deletion. Forward and reverse strands of gRNAs were designed and annealed together to have BbsI restriction site overhangs. gRNAs were then cloned into the pCDF3 cloning vector. Single stranded homologous bridges were generated with 80 bp homologous regions flanking each side of the deletion. An AscI restriction cut site was incorporated into the homologous bridge to facilitate screening. For every deletion, all four gRNAs were injected into *Drosophila* embryos at 125ng/ul each for a total of 500ng, along with 100ng/ul of homologous bridge oligos. Single adult males were then crossed with balancer stocks (*yw* ; *if* / *cyo* ; +), and the progeny were screened for the deletion via PCR. Homologous bridges, gRNAs, and PCR screening primers are shown in Table S5.

Otd/Dve binding site knockout

Otd/Dve binding site knockouts for *outer enh* and *yR7 enh* were generated using site-directed mutagenesis, where the K50 homeodomain consensus sites (TAATCC) were replaced with AAAAAA. Constructs were integrated into the genome and *Drosophila* strains were established using the same methods as described above.

Electrophoretic Mobility Shift Assay

Binding assays were performed as previously described (Johnston et al., 2011; Li-Kroeger et al., 2008).

Probes tested were as follows (bold/underline indicates K50 Otd/Dve site or mutated K50 Otd/Dve site):

yR7 enh 1 5' –CGTGTTAGCCAAACCT**TAATCC**AGGCTAAACGAGGG- 3'
yR7 enh 2 5' –AAATACGCTTATGTC**GGATTA**TCCCATAATTTATG- 3'
yR7 enh mutant 1 5' –CGTGTTAGCCAAACCT**TGCGCC**AGGCTAAACGAGGG- 3'
yR7 enh mutant 2 5' –AAATACGCTTATGTC**GGCGCA**TCCCATAATTTATG- 3'
outer enh 1 5' –AGCAAACAACAAAA**GGATTA**AGTCCAAGACACAC- 3'
outer enh 2 5' –ATACTTATTT**CATTAGGATTA**TTTTTACTAACAT - 3'
outer enh 3 5' –TCACGGCATTAAATT**TAATCC**GCTTAAAAGTTTCA - 3'
outer enh 4 5' –TCACACAAGGATTCG**TAATCC**TTGCGAGGGACCCA- 3'
outer enh mutant 1 5' –AGCAAACAACAAAA**GGCGCA**AGTCCAAGACACAC- 3'
outer enh mutant 2 5' –ATACTTATTT**CATTAGGCGCA**TTTTTACTAACAT- 3'
outer enh mutant 3 5' –TCACGGCATTAAATT**TGCGCC**GCTTAAAAGTTTCA- 3'
outer enh mutant 4 5' –TCACACAAGGATTCG**TGCGCC**TTGCGAGGGACCCA- 3'

Antibodies

Antibodies and dilutions used were as follows: mouse anti-prospero (1:10)(DSHB), rat anti-Elav (1:50)(DSHB), sheep anti-GFP (1:500), mouse anti-Rh3 (1:100)(gift from S. Britt, University of Colorado), rabbit anti-Rh4 (1:100)(gift from C. Zuker, Columbia University), mouse anti-Rh5 (1:2000)(Tahayato et al., 2003), rabbit anti-Rh6 (1:2000)(Tahayato et al., 2003), guinea pig anti-Ss (1:200)(Gift from Y.N. Jan, University of California, San Francisco), rabbit anti-Dve (1:500)(Nakagoshi et al., 1998). All secondary antibodies were Alexa-conjugated (1:400) (Molecular Probes).

Retina dissection and immunohistochemistry

Retinas were dissected and stained as described previously (Hsiao et al., 2012). Larvae were collected and dissected in ice cold PBS (1x), and retinas were isolated using forceps before fixing for 20 minutes in 4% formaldehyde at RT. Samples were washed three times with PBX and kept in primary antibodies diluted in PBX overnight at 4°C. After three washes with PBX, secondary antibodies diluted in PBX were added, and samples were kept at RT for at least 2 hours. After three more washes, samples were kept in PBX at room temperature overnight, before being mounted flat in Vectashield (Vector Laboratories).

To facilitate pupae collection at the desired mid-pupae stage, flies were raised at 25°C in a 12hr light/12hr dark cycle incubator. Pupae heads were dissected in ice cold PBS (1x) and eye-brain complexes were extracted via pipetting. Fixing, antibody staining and mounting procedures were consistent with those of larvae, but pupal retinas were not isolated from the brain until prior to mounting.

Adult flies were anesthetized on CO₂ pads before their heads were removed using forceps. Fly heads were dissected in ice cold PBS (1x), and retinas were isolated using forceps. Fixing and antibody staining procedures were consistent with those of larvae and pupae, although laminae were not removed until after fixing. Retinas were then mounted using SlowFade Gold Reagent (ThermoFisher Scientific).

For all stages of fly development, samples stained with antibodies were visualized under a Zeiss LSM 700 confocal microscope.

Quantification

Fluorescence intensity of nuclear GFP expression of single retinas was quantified using the ImageJ processing program. A small region in the center of each nucleus was selected for fluorescence intensity measurement. Images were taken under subsaturating conditions and comparisons of GFP intensity were drawn between cells of the same retina. Column scatterplots were generated using Graphpad Prism.

Table S1. *dve enh>GFP* Constructs and Primers

Construct	Primers	Restriction sites
<i>yR7 enh</i>	agtcggcgcgcccacaaccatttactcctgc agtcggtacccttctcccagcttcgaatg	<i>AscI</i> <i>KpnI</i>
<i>outer enh</i>	agtcggcgcgccctcatcctcatccctacctac agtcggtaccacaactgcctttgccttg	<i>AscI</i> <i>KpnI</i>
<i>yR7 enh extended to right</i>	agtcggcgcgccgcctagctaccgtgatcaac agtcggtaccgtttagctcgattacgcttc	<i>AscI</i> <i>KpnI</i>
<i>dve min promotor</i>	agtcagatcttgatctggctctctggactc agtcggtaccgtgggaaagtgttgtaagc	<i>BglII</i> <i>BamHI</i>
<i>weak yR7 enh</i>	agtcggcgcgcccggcagcaggtgagttgag agtcggtaccctacgatgacaccgataagcg	<i>AscI</i> <i>KpnI</i>
<i>dorsal R7 enh</i>	agtcggcgcgcccataatcacaacacgagtcgg agtcggtaccgatgggtggcttaactcaatc	<i>AscI</i> <i>KpnI</i>
<i>all PR enh 1</i>	agtcggcgcgccgcttatctgcggctttgtgg agtcggtaccctcgtctgtcccattcca	<i>AscI</i> <i>KpnI</i>
<i>all PR enh 2</i>	agtcggcgcgccgctagcgcatagagcatagatg agtcggtaccgttgctggcaccaatacacg	<i>AscI</i> <i>KpnI</i>
<i>all PR enh 3</i>	agtcggcgcgccgctgctgcctacaagttgga agtcggtaccgccttctgaagactagcac	<i>AscI</i> <i>KpnI</i>
<i>all PR enh 4</i>	agtcggcgcgcccgaactcctcgactcacac agtcggtaccccaattcgtgattg	<i>AscI</i> <i>KpnI</i>
<i>dve enh 1</i>	agtcggcgcgcccactgacatcaattaccgctc agtcggtaccaggagaaaggagtgagttcg	<i>AscI</i> <i>KpnI</i>
<i>dve enh 2</i>	agtcggcgcgccccatccccttagagagctttg agtcggtaccctgtatctggggaatcggatg	<i>AscI</i> <i>KpnI</i>
<i>dve enh 3</i>	agtcggcgcgccgcccacaatgtcaagcatcaaag agtcggtaccacttcccacagtatcatcttg	<i>AscI</i> <i>KpnI</i>
<i>dve enh 4</i>	agtcggcgcgcccagagctgaactgaacaatc agtcggtaccctgtctctgcgctttgtga	<i>AscI</i> <i>KpnI</i>
<i>dve enh 5</i>	agtcggcgcgccgcttagtgagctactgtt agtcggtaccgaaggcttacgaaactaatg	<i>AscI</i> <i>KpnI</i>
<i>dve enh 6</i>	agtcggcgcgcccagctcgtaagcataagca agtcggtaccctgtcccgaattaccctatc	<i>AscI</i> <i>KpnI</i>
<i>dve enh 7</i>	agtcggcgcgccgtggtggtggcgattcatttg agtcggtaccctaccacaaaactagagcacc	<i>AscI</i> <i>KpnI</i>

Table S2. *Drosophila* reagent descriptions

Name	Description	Source
<i>otd^{uvi}</i>	hypomorphic allele, fails to produce protein product in the eye	(Vandendries et al., 1996)
<i>FRT40 sal^{Df(2L)32FP5}</i>	a deficiency that removes the <i>sal</i> gene	(Barrio et al., 1999)
<i>FRT42d dve¹⁸⁶</i>	Dve protein null mutant	(Terriente et al., 2008)
<i>FRT40 GMR-hid, cL</i>	eye-specific enhancer driving <i>hid</i> , an activator of apoptosis	Bloomington
<i>FRT42d GMR-RFP</i>	eye-specific enhancer driving RFP	Bloomington
<i>ey-FLP</i>	eye-specific enhancer driving flippase	Bloomington
<i>ss^{d115.7}</i>	Ss protein null mutant	(Duncan et al., 1998)
<i>ss^{Df(3R)Exel7330}</i>	Deficiency covering the <i>ss</i> locus	Bloomington
<i>UAS-Sal</i>	UAS enhancer driving <i>Sal</i>	(Kuhnlein and Schuh, 1996), (Wernet et al., 2003)
<i>UAS-Dve</i>	UAS enhancer driving <i>Dve</i>	(Nakagoshi et al., 1998)
<i>UAS-Ss</i>	UAS enhancer driving <i>Ss</i>	(Duncan et al., 1998)
<i>IGMR-Gal4</i>	eye-specific enhancer driving <i>Gal4</i>	Bloomington
<i>dve^{Exel}</i>	deletion that removes the first exon of <i>dve</i> , <i>dve-A</i> promoter, and <i>dve yR7</i> enhancer element	See footnote*
<i>dve^{E181}</i>	deletion allele for the <i>dve-A</i> promoter	(Nakagawa et al., 2011)
<i>UAS-nlsGFP</i>	UAS driving nuclear GFP	Bloomington

*We generated the *dve^{exel}* deletion by using hsFLP-mediated recombination between two FRT sites, inserted by P-elements P(XP)d05100 and P(XP)d08355.

Table S3. *Drosophila* shortened and complete genotypes

Shortened	Complete genotype	Figure
<i>dve enh>GFP</i>	<i>yw ; + ; dve enh>GFP</i>	2B-E, 3A, 5A, S1H-Q, S2E-L
all PRs>Ss	<i>yw ; IGMR>Gal4, UAS>Ss ; dve enh>GFP</i>	3E, 5D
all PRs>Sal	<i>yw, UAS>sal ; IGMR>Gal4 ; dve enh>GFP</i>	3G
all PRs>Dve	<i>yw ; IGMR>Gal4 ; dve enh>GFP/ UAS>dve</i>	4A, 6A
<i>sal</i> mutant	<i>yw ; sal^{Df(2L)32FP5}FRT40 GMR>hid FRT40 ; dve enh>GFP/ey>Flp</i>	3F, 5C
<i>otd</i> mutant	<i>otd^{uvi} ; + ; dve enh>GFP</i>	3B, 5B
<i>dve</i> mutant	<i>ey>FLP ; FRT42d dve¹⁸⁶/ FRT42d GMR>RFP ; dve enh>GFP/ +</i>	4B-E, 6B-C
<i>ss</i> mutant	<i>yw ; + ; dve enh>GFP, ss^{BL7985def}/ ss^{d115.7}</i>	3C
all PRs>Ss and Sal	<i>yw, UAS>sal ; IGMR>GAL4, UAS>ss ; dve enh>GFP</i>	3H
<i>otd</i> mutant, all PRs>Ss	<i>otd^{uvi} ; IGMR>GAL4, UAS>ss ; dve enh>GFP</i>	S4A
<i>dve-A del</i>	<i>yw ; FRT42d dve¹⁸⁶/ dve^{E181} ; +</i>	S1A-C

Table S4. *Janelia* and VDRC Gal4 stock numbers

Janelia GMR			
49373	49927	48655	46230
45702	50133	45682	46238
45284	46241	50066	48150
41238			
VDRC Stock			
020724	020725	020737	020739

Table S5. Primers for CRISPR

<i>dve-B del</i>	
Homologous bridge	ttttatggatcgcttggcattataatgaacagcggcgctcgccggctggccatgggcgcatggcgcgcccattgggagcaagttggagctgggcaagccccacatcccatccgcccactgacctaacgc
dveBgRNA1 F	gtcgtggccatgggcgcataat
dveBgRNA1 R	aaacattatgcgcccattggccagc
dveBgRNA2 F	gtcgggataagtacggtgcatgg
dveBgRNA2 R	aaacctatgcaccgtacttatccc
dveBgRNA3 F	gtcgtcatccttccagtgccat
dveBgRNA3 R	aaacatgggcactggaaggatgac
dveBgRNA4 F	gtcgggtgtctgccactgttgaac
dveBgRNA4 R	aaacgtcaacagtggcagacacc
DveBscr F	gctgttgggagattaagttt
DveBscr R	tgcttctgaagactagcac
<i>outer enh del</i>	
Homologous bridge	gctgcctgggcgtcctttctcgggcacttgatagaatttgacaaattgaaaatcctttggcgcgccgaagcctacttaagtccttgaaatccttgagattttgactggtcaagcaatgataa
outergRNA1 F	gtcggacaaccgctcgccacaaa
outergRNA1 R	aaactttgtggcgagcggttgtcc
outergRNA2 F	gtcgttcaagagtccaggcgacc
outergRNA2 R	aaacggtcgctggactcttgaac
outergRNA3 F	gtcgaataagcaatagtctta
outergRNA3 R	aaactaagactattgcttaattc
outergRNA4 F	gtcggacttaagtaggcttcca
outergRNA4 R	aaactgggaagcctacttaagtcc
outer-scr F	ccagtgattatgtatggtc
outer-scr R	gagtgattgggtatttagg
<i>yR7 enh del</i>	
Homologous bridge	acttgctccccgtccgtcgatcgattcaaattaccagcgatttattggcgatcgccagccggcgccgcccgtatggcaatgcaaacagggtgaggggaattactgtcctagacaactttgcagtcagc
yR7gRNA1 F	gtcgttgatcacggtagctagcc
yR7gRNA1 R	aaacgcctagctaccgtgatcaac
yR7gRNA2 F	gtcgtgttcgataacgctggtc
yR7gRNA2 R	aaacgaccagcgttatgcaaacac
yR7gRNA3 F	gtcgttagctcgattacgcttc
yR7gRNA3 R	aaacgaagcgtaatcgagctaaac
yR7gRNA4 F	gtcgtttgattgcatagctac
yR7gRNA4 R	aaacgtagctatggcaatgcaaac
yR7-scr F	gatggctaattggcgagagga
yR7-scr R	gcaatctggcactcccgtt